DEVELOPMENT OF A SMART PROBE DETECTION PLATFORM FOR CANCER DIAGNOSIS

BY

YUSUF BASIRU OLAYINKA

A Thesis Presented to the
DEANSHIP OF GRADUATE STUDIES

KING FAHD UNIVERSITY OF PETROLEUM & MINERALS

DHAHRAN, SAUDI ARABIA

In Partial Fulfillment of the
Requirements for the Degree of

MASTER OF SCIENCE

In

CHEMISTRY

MARCH 2018

KING FAHD UNIVERSITY OF PETROLEUM & MINERALS

DHAHRAN- 31261, SAUDI ARABIA

DEANSHIP OF GRADUATE STUDIES

This thesis, written by **YUSUF BASIRU OLAYINKA** under the direction of his thesis advisor and approved by his thesis committee, has been presented and accepted by the Dean of Graduate Studies, in partial fulfillment of the requirements for the degree of **MASTER OF SCIENCE IN CHEMISTRY**.

Dr. Sulayman A. Oladepo
(Advisor)

26/3/2018

Dr. Abdulaziz Alsaadi
Department Chairman

Dr. Abdalla M. Abulkibash
(Member)

Dr. Salam A. Zummo
Dean of Graduate Studies

Dr. Basheer Chanbasha
(Member)

28/3/18

Date

© Yusuf Basiru Olayinka

2018

Dedicated to my family

ACKNOWLEDGMENTS

I wish to acknowledge my sincere gratitude to all those who have rendered their support in various ways in the preparation of this thesis. First to my advisor (Dr. Sulayman A. Oladepo) and members of my thesis committee (Dr. Basheer Chanbasha and Dr. Abdalla M. Abulkibash) for being supportive during the course of this research.

I wish to acknowledge KFUPM institution for the scholarship granted to me to pursue this master degree. I would like to extend my gratefulness to all faculties in the department of chemistry for their academic and moral support.

My sincere appreciation goes to my father, Mr. Sulayman Yusuf; my mother, Mrs. Balikis Yusuf; and my brother, Mr. Taoreed Yusuf for their moral support and also for their unique model of guidance. May Allah reward them abundantly. Further, I wish to thank the host Kingdom of Saudi Arabia and the Nigeria community for their unique model of support and guidance. Thank you all.

TABLE OF CONTENTS

ACKNOWLEDGMENTS ..... **V**

TABLE OF CONTENTS ..... **VI**

LIST OF TABLES ..... **VIII**

LIST OF FIGURES ..... **IX**

LIST OF ABBREVIATIONS ..... **XII**

ABSTRACT ..... **XIII**

ملخص الرسالة ..... **XV**

CHAPTER 1 INTRODUCTION **1**

1.1 Introduction to MicroRNA **1**

1.1.1 miRNA Biogenesis and Function **2**

1.2 miRNA Implication in Human Disease **4**

1.2.1 miRNA as Oncogene and Tumor Suppressor Genes **5**

1.3 miRNA and Their Application in Therapeutics **8**

1.4 miRNA Detection Methods **9**

1.5 Objectives **15**

CHAPTER 2 LITERATURE REVIEW **16**

2.1 miRNAs Hybridization and denaturation **16**

2.2 Oligonucleotide Probes and Hybridization **17**

2.3 Applications of Oligonucleotide Probes **17**

2.4 miRNA Detection Technologies Developed in this Thesis **18**

2.5 How Smart Probes Work **21**

CHAPTER 3 EXPERIMENTALS 23

3.1 Introduction 23

3.2 Materials and Reagent 23

3.3 Fluorescence Measurements 26

CHAPTER 4 RESULTS AND DISCUSSION 30

4.1 Design of the Smart Probes for the detection of miR-21 target 30

4.2 Thermal Transition Profile 32

4.3 Enhanced Temperature-Dependent Discrimination 35

4.4 Hybridization Kinetics Measurements 37

4.5 Concentration-Dependent Measurements 40

CHAPTER 5 DETECTION OF LET-7A CANCER BIOMARKER USING A SMART PROBE 43

5.1 Design of a Smart Probes for the detection of Let 7 target 43

5.2 Thermal Transition Profiles 45

5.2.1 Thermal Transition Profile in the Absence of Blockers 45

5.2.2 Thermal Transition Profile in the Presence of Blockers 48

5.3 Enhanced Temperature-Dependent Measurements 52

5.4 Concentration-Dependent Measurements 53

5.5 Comparison of the Developed Method to Prior Methods 56

CHAPTER 6 CONCLUSION 57

REFERENCES 59

VITAE 70

LIST OF TABLES

Table 3.1: List of oligonucleotide sequences for miR-21. 25

Table 3.2: List of oligonucleotide sequences for Let-7. 26

LIST OF FIGURES

Figure 1.1: miRNA biogenesis. miRNA is at first encoded in genomic DNA. It experiences transcription, trailed by a progression of prepared ventures to produce mature miRNA, which ties to mRNA, repressing protein translation. Adapted from Cissell *et al*. (2007). ..... …3

Figure 1.2: A fundamental model of miRNAs going about as tumor suppressors and oncogenes proposed by Garzon *et al.* [90]..... 6

Figure 1.3: Hairpin-probe miRNA detection. Molecular beacons consisting of a stem loop in absence and presence of miRNA target. The target hybridizes with loop, separating the stem, resulting in an increase in fluorescence intensity. 13

Figure 2.1: How Smart probes Work..... 22

Figure 3.1: Picture of FLS 920 fluorescence spectrometer setup. 28

Figure 4.1: Structure of the SP and that of SP-RNA1 duplex and their T_m. The sequence of the miR-21 target is also shown (top right). setup..... 31

Figure 4.2: Thermal transition profiles of SP (black), SP-RNA1 (red), SP-RNA2 (green) SP-RNA2b (blue), SP-RNA3 (cyan) and SP-RNA4 (magenta) sequences. Each measured fluorescence intensity has been normalized of the intensity at 78 ^{o}C..... 33

Figure 4.3: The miR-21 sequence discrimination at 56 ^{o}C. This data was extracted from from thermal transition profile and the raw signal for SP alone was substracted from those of SP-target signals. 36

Figure 4.4: Time-dependent fluorescence signal of SP-RNA1 incubated at 22.5 ^{o}C..... 38

Figure 4.5: Time-dependent fluorescence signal of SP-RNA1 incubated at 37 ^{o}C. 39

Figure 4.6: Linear portion of the Calibration plot for the detection of miR-21 sequence. 41

Figure 4.7: Concentration-dependent plot for 100 nM SP in the presence of different concentrations of RNA1 (0-1000 nM). Curve becomes non-linear beyond 100 nM RNA1 target concentration. 42

Figure 5.1: Structure of the SP and that of SP-Let 7a hybrid and their melting temperatures. The stem sequences of the SP are underlined in the SP-Let7a hybrid (bottom right) for easy correlation with the structure of the SP on the left. The Let-7a target sequence is also shown (top right). 44

Figure 5.2: Thermal transition profiles of SP (black), SP-Let 7a (red), SP-Let7b (green) and SP-Let7c (blue), target sequences. Each measured fluorescence intensityhas been normalized to the intensity at 78 ^{o}C. 46

Figure 5.3: Thermal transition profiles of SP (black), SP-Let 7a (red), SP-Let7b in the presence of let-7b blockers (green) and SP-Let7c hybrid in the presence of let-7c blockers (blue). Each measured fluorescence intensity has been normalized to the intensity at 78 ^{o}C. Each of these four curves represent a separate experiment. 49

Figure 5.4: Thermal transition profiles of SP (black), SP-Let7a (red), SP-Let7a-let7b-let7c without blockers (green), and SP-Let7a-let7b-let7c in the presence of 7b and 7c blockers (blue). Each measured fluorescence intensity has been normalized to the intensity at 78 ^{o}C. This is a single-pot experiment where SP-Let-7a, was measured in the presence of let-7b and let-7c and their corresponding blockers. 51

Figure 5.5: The Let-7 sequence discrimination at 20 ^{o}C. This data was extracted from thermal transition profiles (Figure 5.3). 53

Figure 5.6: Linear portion of the Calibration plot for the detection of Let-7a sequences. 54

Figure 5.7: Concentration-dependent plot of 100 nM SP in the presence of different concentrations of Let-7a (0-1000 nM). Curve becomes non-linear beyond 5 nM Let-7a target concentration. 55

LIST OF ABBREVIATIONS

6-FAM	:	6-carboxy fluorescein
DNA	:	Deoxyribonucleic acid
LNA	:	Locked nucleic acid
MBs	:	Molecular beacons
RNA	:	Ribonucleic acid
miRNAs	:	MicroRNAs
mRNA	:	Messenger RNA
PCR	:	Polymerase chain reaction
Pri-miRNA	:	Primary microRNA
piRNAs	:	Piwi-interacting RNAs
pre-miRNA	:	Precursor microRNA
qRT-PCR	:	Quantitative reverse transcription-PCR
RT-PCR	:	Real-time reverse transcription-PCR
RISC	:	RNA-induced silencing complex
siRNA	:	Small interfering RNA
SPs	:	Smart probes

ABSTRACT

Full Name : Yusuf Basiru Olayinka

Thesis Title : Development Of A Smart Probe Detection Platform For Cancer Diagnosis

Major Field : Chemistry

Date of Degree : March, 2018

MicroRNAs (miRNA) expression play crucial roles in many physiologic and pathologic processes and are significant biomarkers for human cancer. This has fueled the need for the development of highly sensitive and selective detection methods for miRNAs. However, rapid, low cost, selective and sensitive detection of miRNAs remain a challenge due to their short lengths, low abundance, and sequence homology. Current detection platform of microarray, PCR and Northern blotting suffer from drawbacks including being time-consuming, low sensitivity and lack of simplicity. This work mainly focuses on developing a selective and sensitive hairpin smart probe (SP)-based methods for specific detection of selected microRNA (miRNA) target sequences. The loop sequence of each smart probe is perfectly complementary to the miRNA sequence of interest. The stem of these self-quenching SP contains a fluorophore on one end and a set of guanine bases on the other end are used as quenchers. The fluorescence of the SP is quenched by the guanine bases at room temperature and in the absence of the target. The SP recognizes the miRNA target sequence and it switches on its fluorescence as a result of the spontaneous hybridization of the SP with the target. The SP successfully discriminated between the perfect miRNA target and mismatch sequences. This new SP-based method does not involve any amplification steps. When the SP was incubated with

the miRNA at 37 ^{o}C, the hybridization kinetics took only 40 minutes compared to room temperature that takes around five hours to complete. In addition, these new SPs have exquisite sensitivity and give a limit of detection (0.53 and 0.02 nM) and limit of quantitation (1.76 and 0.07 nM) for miR-21 and Let-7a respectively. This detection method represents a simple, fast, specific and potential diagnostic tool for the various human cancers caused by miRNA.

ملخص الرسالة

الأسم بالكامل: يوسف بشير اولينكا

عنوان البحث: تطوير جهاز كشف مجس ذكي لتشخيص السرطان

التخصص: كيمياء

تاريخ الدرجة: مايو، 2018

تلعب جزيئات RNA الدقيقة دورا مهما في كثير من العمليات الفيسولوجية وعلم الأمراض وتعتبر مؤشرات حيوية مهمة لامراض السرطان التي تصيب الانسان، وذلك دعم الحوجة لتطوير طرق ذات حساسية وانتقائية عاليتين للكشف عن لجزيئات RNA الدقيقة، ولكن ايجاد طريقة سريعة، ذو كلفة منخفة، انتقائية و حساسة للكشف عن هذه الجزيئات يظل تحديا نسبة لقصر الطول، قلة الوفرة و تماثل التسلسل. جهاز الكشف التياري للمصفوفات الدقيقة، PCR و جهاز التشرب الشمالي، كل هذه الطرق تعاني من مشكلة استهلاك الوقت، قلة الحساسية و تعقيد الطريقة. هذا البحث يركز على تطوير مجس دبوس ذو انتقائية وحساسية عالية لكشف النوعي لجزيئات RNA الدقيقة. التسلسل الحلقي لكل مجس ذكي يكون متكامل بطريقة مثالية مع تسلسل جزئ الRNA ذو الاهتمام. يحتوي المجس الذكي ذو خاصية التثبيط الذاتي على فلوروفور في نهاية ومجموعة من قواعد كونين في النهاية الاخرى وتستخدم كمثبطات. يتم تثبيط المجس الذكي بواسطة قواعد الكوينين عند درجة حرحاة الغرفة في غياب المادة الهدف. يقوم المجس بتميز تسلسل الهدف لجزئ الRNA الدقيق و يتم تفعيل الفلورة نتيجة للتهجين التلقائي للمجس مع المادة الهدف. يقوم المجس بالتفريق بين جزئ الRNA الدقيق المثالي و التسلسل غير المتطابق. هذه الطريقة، طريقة المجس الذكي لاتحتاج اي خطوات لتضخيم الاشارة. عندما يتم تحضين المجس مع جزئ الRNA الدقيق في درجة حرارة 37^{o} C ، حركية التهجيت تتطلب 40 دقيقة فقط مقارنة مع درجة حرار الغرفة التي تتطلب حوالي خمس ساعات لاتمام العملية. بالاضافة لذلك تتمتع هذه العملية بحساية ممتازة وحد كشف (0.53 and 0.02 nM) وحد التكميم (1.76 and 0.07 nM) لmiR-21 و Let-7a على التوالي. هذه الطريقة تمثل طريقة بسيطة، سريعة، انتقائية و اداة تشخيص لمختلف امراض السرطان التي تحدث بسبب جزيئات الRNA الدقيقة

CHAPTER 1

INTRODUCTION

1.1 Introduction to MicroRNA

Micro-RNAs (miRNAs) are non-coding single-stranded RNA molecules that regulate several physiological and pathological processes [1-2]. Recent studies have found that the dysregulation of miRNA expression is closely associated with several diseases including lung cancer, hepatocellular carcinoma, pancreatic cancer, breast cancer and gastric carcinoma [3-6]. In addition, they play an important role in many biological processes and recognized as biomarkers in clinical diagnosis and therapy [7]. Consequently, miRNAs are regarded as new oncogenes or tumor suppressor genes and new biomarkers for the diagnosis and prediction of treatment response and prognosis [8-10]. As microRNAs are an important class of gene regulators in vivo, the specific and sensitive detection of microRNAs has become more and more important [11]. The detection of miRNAs is quite challenging due to their high homology, small size and low abundance among miRNA family members [12].

MicroRNAs were the primary endogenous little RNAs to be found [1, 13–16]. While doing hereditary examination of formative mutants of *Caenorhabditis elegans*, Ambros, and his group observed that the translation of lin-14 mRNA into LIN-14 protein was repressed amid its formative stage change by a little transcript of 22 nucleotides in length

[17]. Around a similar time, Ruvkun and his group watched a comparable marvel [17], in spite of the fact that Ruvkin's inquires about concentration was lin-14 gene, while Ambros' examination was on the lin-4 gene. In 1993, by joint endeavor of Ambros and Ruvkun groups, the main miRNA lin-4 was discovered [14, 17]. Seven years after the discovery of the first miRNA, the second miRNA, let-7 was found in *C. elegans* by Reinhart *et al.* [18] in 2000. It has been demonstrated that conversely with lin-4, the let-7 sequence is preserved crosswise over species from flies to people [19]. This finding affected the investigation of miRNAs in other organisms [19] and provoked a rebellion in the explanation of this new class of small noncoding RNAs called miRNAs. Since then, a large number of miRNAs have been identified in humans, worms and Drosophila [20-21]. Gene regulation by miRNAs plays a role in cell multiplication, cell demise, and tumorigenesis and in addition mammalian cell improvement [22-23].

1.1.1 miRNA Biogenesis and Function

It has been established that a multi-step process is important to create a developing type of miRNA [24]. miRNA biogenesis begins in the nucleus and in the end, brings about mature miRNA in the cytoplasm (Figure 1.1). Before mature miRNA is formed, primary miRNA (pri-miRNA), a long strand of RNA containing stem-loop structures (up to 1kb in length), is at first transcribed by RNA polymerase II [25], and further excised by the endonuclease Drosha [26]. After excision, the former pri-miRNA, termed pre-miRNA, is exported to the cytoplasms by the RNA-binding protein Ran-GTP and the exporter receptor Exportin-5 [27–29]. This pre-miRNA comprises of a long stem of roughly 25-30 bp alongside a small loop structure. After the pre-miRNA is released from the Exportin-5, it is cleaved by an RNase III enzyme known as Dicer, to generate mature miRNA. The

mature miRNA is further incorporated with the RNA-induced silencing complex (RISC), consisting of proteins from the Argonaute family, by which the

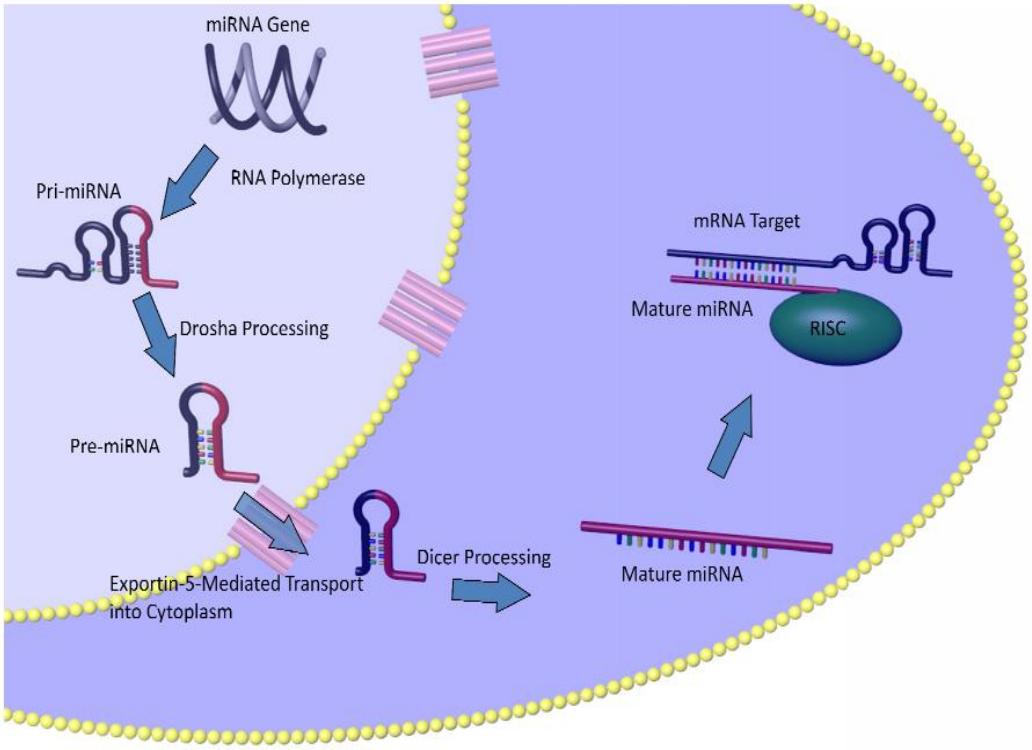

Figure 1.1: miRNA biogenesis. miRNA is at first encoded in genomic DNA. It experiences transcription, trailed by a progression of prepared ventures to produce mature miRNA, which ties to mRNA, repressing protein translation. Adapted from Cissell *et al*. (2007).

miRNA anneals to the 3' untranslated region of its complementary target messenger RNA (mRNA) [30-31]. Once bound to the target mRNA, the miRNA can induce cleavage of the mRNA, regulating protein translation directly, or regulating translation indirectly by remaining bound to the mRNA. Because of the similarities between small interfering RNA (siRNA), miRNA, and piwi-interacting RNAs (piRNAs), it is important to differentiate between each of these small RNAs. While each of the three is about a

similar length, they are handled distinctively in the cell. Every one of the three is generated by RNase enzymes Dicer and Drosha. The cleavage of exogenous long dsDNA precursors in response to viral infections or artificial introduction generates small interfering RNAs (siRNAs), whereas the processing of genome-encoded stem-loop structures generates miRNAs. A recently uncovered class of small RNAs called piwi-interacting RNAs (piRNAs) is slightly longer than miRNAs (~26-31 nucleotide) [32]. The proteins required for this pathway are unknown but it is known that the piRNAs function to silence transposons through a complex amplification process that can even modify histones and carry out DNA methylation [33-35].

1.2 miRNA Implication in Human Disease

MicroRNA has been associated with various diseases, including malignancy. It assumes a vital part in cell science, including apoptosis, multiplication and pathological process [36–39]. Also, miRNAs are involved in different cellular activities, for example, insulin secretion [38], viral replication [41–43], neurotransmitter synthesis [42], and resistant reaction [43]. It can be found freely circulating in bodily fluids, for example, serum [44], urine [45] and saliva [46]. The utility of circulating miRNA as cancer biomarkers, therefore, would be highly advantageous in terms of developing rapid diagnostic tools.

As the investigation of miRNA expands, more and more researchers are finding links between miRNA expression levels (the amount of miRNA in the cells) and the onset of cancer and other diseases [47]. Various studies have found that miRNA expression levels are increased (upregulated) or decreased (downregulated) in cancer cells. For instance, miR-15a and miR-16-1 are downregulated in B-cell chronic lymphocytic leukemia [48];

miR-143 and miR-145 are downregulated in breast, prostate, cervical, and lymphoid cancer cells [49]; while miR-21, miR-373, and miR-520c are upregulated in breast cancer cells [4, 52], and miR-184 is upregulated in prostate cancer cells [51]. There are certainly hundreds of more miRNAs which are linked to cancer and the list grows larger as more and more studies are performed. Along with cancer, miRNAs have appeared to play a vital role in cardiovascular disease. Hammond and colleagues have discovered that in the presence of mutated Dicer, the enzyme which cuts pre-miRNA into mature miRNA, the miRNA which is essential for cardiovascular health cannot be processed. This ultimately results in progressive dilated cardiomyopathy, which prompts heart failure, and eventually death [52]. Because of the significance of miRNA in disease, it is important to develop miRNA based diagnostic and therapeutic techniques. Because of their widespread gene regulation and their effects on human wellbeing, miRNAs have garnered much attention in the biomedical field.

1.2.1 miRNA as Oncogene and Tumor Suppressor Genes

Due to the common characteristic that was observed in miRNA expression patterns, it has been suggested that deregulation of these miRNAs were not caused by random events in cancer. This led to the assumption that up-regulated miRNAs may act as oncogenes and down-regulated miRNAs may act as tumor suppressors [55–58]. miRNAs also function as tumor suppressors in different cancer types by regulating the oncogenic process and preventing tumor development. Kefas *et al.* documented the association of EGFR and AKT pathway activation with the aggressiveness of glioblastoma [56]. Figure 1.2 represents the basic model of miRNAs acting as tumor suppressors and oncogenes proposed by Garzon *et al.* [54]. They proposed that, when a miRNA down-regulates the

expression of an oncogene, it can be categorized as a tumor suppressor and is frequently observed to be lost in tumor cells. The loss of function of these miRNAs may occur due to any abnormality in the miRNA biogenesis, such as mutation, deletion or promoter methylation. These might produce an abnormal expression of the target oncogene, which then contributes to tumor formation, which will ultimately induce cell proliferation,

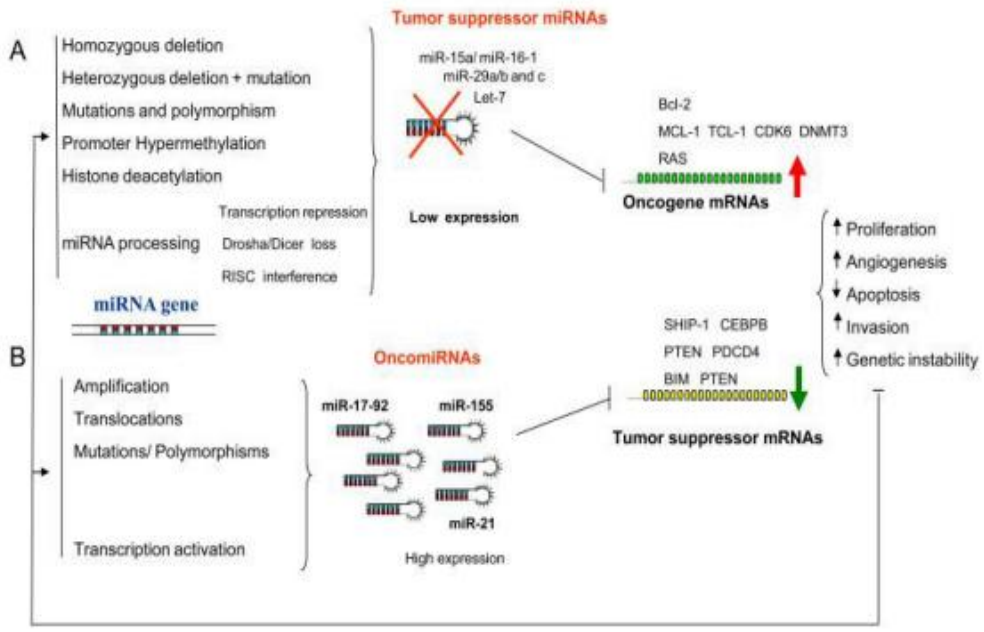

Figure 1.2: A fundamental model of miRNAs going about as tumor suppressors and oncogenes proposed by Garzon *et al.* [90].

A) When a miRNA down-regulates the expression of an oncogene, it can be sorted as a tumor suppressor and is much of the time seen to be lost in tumor cells. Loss of capacity of these miRNAs may happen because of any anomalies in the miRNA biogenesis, for example, change cancellation or promoter methylation. These might create an anomalous articulation of the objective oncogene, which at that point adds to tumor development, which will, at last, incite cell multiplication, intrusion, angiogenesis, and diminished cell demise.
B) MicroRNA that down-directs tumor silencer qualities can be characterized as an oncogene (oncomiR). In the event that it is overexpressed, it may add to tumor arrangement by angiogenesis and intrusion or by avoiding apoptosis and expanding hereditary insecurity. Adapted from Garzon *et al*. (2010).

invasion, angiogenesis and decreased cell death (Figure 1.2, A). For example, it has been shown by Calin *et al.* that miR-16-1 cluster located in the chromosome 13q14 region is a negative regulator of the B cell lymphoma 2 proteins (BCL2), in patients with chronic lymphocytic leukemia (CLL) due to a genomic deletion of this region [50, 59-60]. On the contrary, if a miRNA that down-regulates a tumor suppressor gene is overexpressed, it might contribute to a tumor formation by angiogenesis and invasion by preventing apoptosis and increasing genetic instability (Figure 1.2, B). It has been reported that overexpression of the oncogenic miRNAs, mir-21, mir-155 and mir-17-92 cluster are linked with tumor initiation and progression by repressing the expression of tumor suppressor genes, such as phosphatase and tensin homologue (PTEN), and programmed cell death 4 (PDCD4) [61–65]. miR-17-92 cluster is one of the first oncogenic miRNAs that was identified by Di Leva *et al*., which consists of seven miRNAs: miR-17-5p, miR-17-3p, miR-18a, miR-19a, miR-20a, miR-19b- 1, and miR-92-1 [62]. The role of miR-17-92 cluster as an oncogene was confirmed by L. He *et al.* in the E μ-Myc transgenic mouse model for B cell lymphoma [49]. Another oncogenic miRNA, miR-21, is up-regulated in almost all types of cancer. Its oncogenic activity was shown by J. Liu *et al*. in transgenic mouse models with alternated miRNA-21 function combined with a mouse model for lung cancer [64]. It should be noted though that miRNA function depends on the expression of its target. Depending on the cell type, some miRNAs could function as oncogenes, as well as tumor suppressors. Presumably, miRNAs are not responsible for a specific phenotype by acting on a single target; instead, they are involved in complex interactions with the transcriptome machinery and can simultaneously target multiple mRNAs. [64].

1.3 miRNA and Their Application in Therapeutics

Because of the increasing correlation of miRNA levels with diseases, it has been suggested to explore various therapeutic options for miRNA function inhibition or delivery of miRNA in cells where the onset of disease may occur if miRNA level is downregulated. In order to achieve these tasks, miRNAs must be relatively examined in both healthy and unhealthy cells. Once a miRNA has been determined to be a suitable biomarker, it will be important to explore options on how to counteract the disease linked to the specific miRNA or miRNAs. In the event that the miRNA levels are too high, a few options to tackle this problem may be used. Anti-sense oligonucleotides which hybridize with the miRNA can be introduced, preventing the target miRNA from hybridizing with the 3' UTR of the mRNA [65]. By doing this, it is possible that abnormal gene regulation will not occur from the target miRNA. A more effective technique to design antisense miRNA is to employ locked nucleic acid (LNA) probes rather than DNA oligonucleotide probes. LNAs contain a 2'-O-4'C methylene bridge on the furanose ring which results in a more rigid double-stranded nucleic acid structure that is more thermally stable as well. This could prevent the separation of the hybrid between target miRNA and antisense oligonucleotide. Additionally, it has been discovered that antagomirs, anti-sense oligonucleotides which were conjugated to cholesterol to aid in cellular delivery, might be useful therapeutic agents for tumors or other diseased cells. In a study by Krutzfeldt and colleagues, it was determined that 7 cholesterol-modified antagomirs injected into mice inhibit miRNA activity [65]. For overexpressed miRNAs

which prompt tumor development, the delivery of antagomirs or antisense LNA probes, coupled with delivery of miRNAs which lead to tumor suppression are ideal [66]. It is additionally conceivable to transfect cells with miRNA in order to inhibit protein translation, rather than to promote protein translation. For example, let-7 miRNA transfection has been shown to reduce tumor growth in cancer cells [69–71]. Introduction of miR16 has also been shown to reduce tumor growth in prostate cancer cells [70]. In order to deliver the therapeutic agents, non-invasive delivery is desired, such as liposomal delivery. Recently, single-walled carbon nanotube (SWNT) delivery based on endocytosis has shown promise as a drug delivery alternative [71]. SWNTs have just appeared to deliver siRNA to cells [74-75], and thus can be applied to miRNA delivery as well. Additionally, the toxicity of SWNT can be substantially decreased by using smaller length SWNTs which are expelled quickly in the urine after use [74]. Prior to these therapeutic methods being used in humans, much research should be performed with respect to miRNA levels in healthy vs. unhealthy cells to guarantee that addition of antagomirs and/or miRNAs will not cause harm in the body by inhibiting or promoting expression of proteins which can bring about the onset of a different type of disease.

1.4 miRNA Detection Methods

Traditional methods for detecting miRNAs include Northern blotting, RT-PCR, microarrays, in-situ hybridization and others [77–79]. Most of the detection methods are based upon hybridization which relies on an optical label in order to translate the hybridization event into a measurable signal. There are label-free methods such as those of Raman spectroscopy [78]. In one particular example, silver nanorods are immobilized

on a substrate and the target nucleic acids are then adsorbed to the nanorods, resulting in Raman signal that is sequence-specific [78]. However, each of these methods has its own individual limitations.

Northern blotting is the standard method for microRNA detection and used for detection of both mature and precursor forms of miRNA since it involves a size-based separation step. The Northern blotting protocol involves miRNA extraction, followed by polyacrylamide gel electrophoresis. Afterwards, separated sample is transferred to the blotting membrane, followed by visualization via hybridization with a complementary radioactively labeled probe [81–83]. A complication is that Northern blotting requires radiolabelling, which can introduce significant contamination, has low sensitivity and require a high amount of samples for miRNA detection [84–87]. Traditional northern blotting sensitivity problem has been minimized with the addition of locked nucleic acid (LNAs) to the probe sequences, increasing the detection sensitivity by almost 10-fold [85].

Quantitative reverse transcription polymerase chain reaction (qRT-PCR) is considered as the current gold standard technology for miRNA detection [76]. It is based on two consecutive and sequence-specific amplification steps of the miRNA of interest. The first step involves the synthesis of complementary DNA (cDNA) from extracted RNA using a reverse transcriptase (RT) enzyme [84]. However, two reactions are carried out, the first uses random primers to reverse transcribe all RNA in the samples to cDNA, which is then used to amplify an endogenous control [86]. The second reaction uses miR-specific RT, which reverse transcribes a single miRNA of interest only, using primers designed as hairpin loops due to miRNA short lengths [87]. qRT-PCR is capable of detecting the

minimal concentration of miR-target because of the two amplification steps. It has good detection efficiency, but they are time-consuming, requires highly purified samples and costly, thus limiting their use [88].

Microarray is another method that can detect miRNA [77]. A widely used strategy for microarray analysis is fluorescent labeling of probe followed by hybridization of miRNA target to capture probes on the array. Like northern blotting, by incorporating LNA in the capture probes to recognize target miRNAs, the specificity of a microarray increases significantly [89]. miRNA microarrays have been used to study the biogenesis of miRNAs, differential miRNA expression profiles, disease characterizations, and stem cell development, to name a few applications [90]. Despite having the benefit of being less expensive and allowing a large number of parallel measurements, microarray lacks specificity, sensitivity and the ability to perform absolute quantification of miRNA abundance, thus limiting their use [91].

The in-situ hybridization techniques can be subdivided into two groups as solid and solution phase hybridization methods. In a solid phase hybridization method, a capture probe is immobilized onto a solid surface to be hybridized with its complementary target [11], while in the solution phase, probe and complementary target are mixed and hybridized with each other [92]. However, this technique requires specialized equipment [93].

A colorimetric detection method based on the use of plasmonic coupling effect has also been used for the detection of miR-21 [94]. Gold nanoplasmonic particles are assembled in a core-satellite configuration in the presence of target miRNA, inducing a remarkable

change in the scattering color and spectra at the picomolar level [95]. This approach works well and provides low detection limit, but a specialized nanotechnology platform is needed [95]. Therefore, development of more efficient and low-cost detection methods is very important. The development of simple and highly sensitive methods with the capability of clinical application also remains a great challenge. Thus, various methods are being developed, such as rolling circle amplification, enzyme repairing amplification and isothermal amplification method [98-99]. All these methods present enhanced sensitivity for miRNA detection, but each of these methods has its own individual limitations. In rolling cycle amplification method, more condition optimization is needed [89], while isothermal amplification has good sensitivity even as low as a single cell, but the required multiple enzymes increase the chance for errors and added costs, thus limiting their use [89]. Consequently, the discrimination of a perfect match (PM) versus a mismatch (MM) still remains a major challenge for probe-based hybridization method. Hence, it is important to design probes with specificity to recognize targets varying at just a single-base position in hybridization assays.

There have been numerous real endeavors to enhance the specificity of probe-based hybridization for single MM separation over the years. In addition to the conventional probes, different kinds of oligonucleotide probes have been developed, and some of them have been successfully demonstrated to achieve discrimination at a level of a single nucleotide MM [98]. One case is “molecular beacon” probes, which are oligonucleotide probes. A molecular beacon (MBs) is a stem-loop hairpin structure consisting of a double strand stem approximately 4-6 base pair in length, containing donor and quencher fluorophore along with a single-stranded loop complementary to the target DNA or RNA

base sequence (Fig 1.3). In the absence of target the fluorescence of the donor is quenched, whereas, in the presence of target, the annealing of the MBs with the target leads to separation of the donor and acceptor fluorophore, resulting in fluorescence emission upon excitation. MBs are also very selective, differentiating targets with as little as a single base mismatch. One of the issues of using MBs for direct nucleic acid detection is no signal amplification, which limits sensitivity [98]. Also, Dual-labelling (fluorophore and quencher) process is relatively complex and expensive to synthesize.

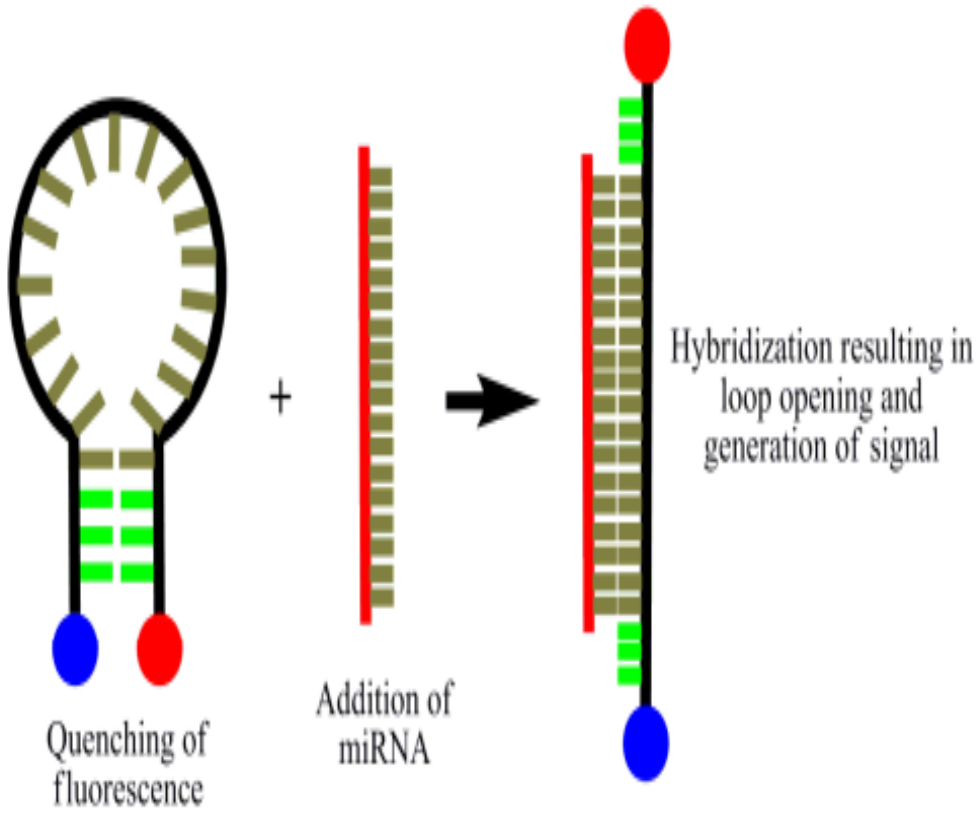

Figure 1.3: Hairpin-probe miRNA detection. Molecular beacons consisting of a stem and loop in absence and presence of miRNA target. The target hybridizes with the loop, separating the stem, resulting in an increase in fluorescence intensity.

Recently, Smart probes (SPs) that take advantages of the selective quenching of fluorophores by neighboring guanine bases were introduced [99]. These probes are oligonucleotide probes just like MBs, but quenching is achieved by photoinduced intramolecular electron transfer upon contact with the guanine residues because of the guanine low oxidation potential [100]. These self-quenching SPs consist of a fluorophore on one end and multiple guanine bases on the opposing end are used as quenchers. Guanine bases were incorporated as part of the stem sequence to act as a quencher of fluorescence emission through interaction with the dye in close proximity. Thus, the main focus of this work is the development and characterization of SPs and to demonstrate their suitability for in vitro and sequence-specific detection of miRNA target sequence. Where necessary, enhancement of sequence-specificity of SPs is achieved by including nucleic acid blockers that are complementary to target sequences containing the mismatches. Thereby, these mismatched, non-targeted sequences are blocked and only the perfectly complementary sequence does consequently open the fluorescently labeled probe. Also, the nucleic acid blockers are straight oligonucleotides with no stem. These studies also show the inherent sensitivity of SPs and demonstrate that this method can accurately recognize even single-base mismatches.

1.5 Objectives

Based on the numerous details explained in the introduction, the major objectives of this work is the design and characterization of the new Smart Probes (SPs) and demonstrate their suitability for in vitro and sequence-specific detection of miRNA target sequences. Another objective of this work is to show the inherent sensitivity of SPs and demonstrate that this method can accurately recognize even single-base mismatches. In order to accomplish this, the precisely planned objectives for this MSc research are highlighted below:

- Development of smart probes suitable for the detection of miR-21 and let-7a targets.
- Characterization of the new smart probes both in the presence and absence of the miR-21 and let-7a targets.
- Demonstrate their suitability for sequence-specific detection of perfect miR-21 and let-7a target sequences and recognizing even single-base mismatches.
- Hybridization kinetics experiments.
- Determination of figures of merit: sensitivity, limit of detection (LOD) and limit of quantitation (LOQ).

CHAPTER 2

LITERATURE REVIEW

2.1 miRNAs Hybridization and denaturation

miRNAs are a class of small, single-stranded, non-protein coding RNA molecules that regulate cellular messenger RNA (mRNA) and protein level by binding to specific mRNAs [101]. mRNA hybridization is a fundamental process that describes the formation of a double-stranded structure from the binding of a single-stranded miRNA to its complement [102]. Based on the rule of Watson-Crick base pairing, the sequences of the two strands have to be complementary for hybridization. This results in the specificity of molecular recognition of one strand by the other via Watson-Crick base pairing during hybridization [103]. The energy release during hybridization is large enough to obtain stable hybrid. In a process termed ‘‘melting’’ or ‘‘denaturation’’ of the duplex, the bonds are disrupted. Denaturation and renaturation of miRNAs can be achieved repeatedly by slow heating and cooling, respectively, without altering the molecular integrity of each strand [101].

2.2 Oligonucleotide Probes and Hybridization

An oligonucleotide probe or a single-stranded DNA sequence is used in a hybridization-related assay to identify target DNA with complementary sequence [101]. It can be utilized to question and distinguish the complementary target DNA in an unknown DNA mixture that may be related in sequence to the probe. The presence of a specific sequence in a DNA sample is generally identified by hybridization using oligonucleotide probe with a complementary sequence. After mixing single strands of the probe with single strands of the target, probe DNA strands and the complementary target DNA strands can hybridize to form probe-target duplexes. [102]

2.3 Applications of Oligonucleotide Probes

Oligonucleotide probes play a significant part in hybridization techniques including RNA interface, polymerase chain reaction (PCR) and microarray [102]. In situ hybridization is a common method for visualizing nucleic acid target within fixed tissue and cell type and is based on a method where RNA probe joined with a marker can hybridize to a specific target [102]. So far, oligonucleotide probes have been applied in various applied and basic research area. They are used for detection and quantification of particular nucleic acids, gene processing analysis, investigation of the relationship among various species and localization of nucleic acids in cells [103]. In medicine and ecological sciences, oligonucleotide probes play a crucial part in the identification of infectious agents, for example: recognition of gene responsible for pathogenesis, fungi, viruses, and bacteria

[98]. In pathology and heredity, they are utilized for hereditary screening of hereditary diseases, the hereditary fingerprint of individuals and determination of the distribution of specific sequences [104]. Also, in agriculture, they are helpful as an instrument for plant breeding [98]. When applied in environmental sciences, rRNA-targeted oligonucleotide probes are used as a part of the direct analysis of microbial population structures of complex natural and engineered frameworks [90].

2.4 miRNA Detection Technologies Developed in this Thesis

Smart probes (SPs) are single-stranded hairpin-shaped oligonucleotide probes [105]. The inherent signaling property of SPs is due to their hairpin conformation [105-106]. The stem of the SPs consists of a fluorophore on one end and multiple guanine bases on the opposing end are used as quenchers. In the absence of complementary target sequences, they form a stem-loop hairpin structure that results in quenching of the fluorophore's fluorescence [107]. Hybridization of the SP's loop sequences with target sequences opens the hairpin and separates the fluorophore from the quenching guanine residues. The structure of our hairpin oligonucleotide probes is analogous to molecular beacon hairpins (MBs) [108-109]. A molecular beacon consists of a single-stranded DNA molecule in a stem-loop conformation with a donor fluorophore and a quencher. A commonly used quencher, 4-(4'-dimethylaminophenylazo) benzoic acid (dabcyl) is a chromophore [109]. Dabcyl, a neutral and hydrophobic molecule can serve as a universal quencher for a variety of fluorophore, but the quencher in MBs is replaced with multiple guanine residues in SPs [50, 106]. Despite the wide applications and the sensitivity and selectivity

of MBs, they have several limitations [110]. Dual-labeling (fluorophore and quencher) process is relatively complex and expensive to synthesize [110]. Thus, in contrast to MBs, SPs are only labeled at one end with a fluorescent dye. The major advantage of SPs as compared to MBs is that unlabelled oligonucleotides are relatively easy to synthesize (single labeling) and have free terminus at the guanosine end for further modification [111]. For instance, MB requires site-specific labeling of each terminus of the hairpin with two extrinsic molecules, a donor, and a quencher [112]. In the SP, the fluorophore is attached to one end of the oligonucleotide and quenched by guanosine residues in the complementary stem via photo-induced intramolecular electron transfer [112-113]. Upon hybridization to the target sequences, the fluorescence is restored due to a conformational reorganization that forces the stem strands apart [89, 105]. The SP is relatively easy to synthesize and have a free terminus at the poly-guanosine end for further modification [99]. Due to the increase in fluorescence intensity upon hybridization, SP has been used for various detection assays. For instance, monitoring of DNA polymerase fidelity [99], detection of UV-induced DNA photodamage [10], and detection of glutathione and cysteine in human plasma and cells [114].

This study developed SPs to recognize miRNAs, with lengths of about 22 nucleotides. The SPs developed were used in homogeneous assays for detecting miR-21 and let-7a, and their analogous single-base mismatch sequences. The miR-21 and let-7a target sequences are specifically recognized by the loops of the individual SPs. Survey of the literature has shown that one of the most widely studied cancer biomarkers is miRNA. In case of cancer, microRNA-21 (miR-21) can act either a tumor suppressor or as oncogenes [3-6]. However, miR-21 has been specifically implicated in several types of cancer,

including breast, lung, prostate, liver, stomach colon, and pancreatic cancer [1-2]. Various techniques have been adopted for the detection of microRNA. For example; Tugba Kilic *et al* [92] successfully used electrochemical-based method for the detection of miR-21 in breast cancer cells. Jiyun Part *et al* [96] used colorimetric platform for detection of miR-21 based on nanoplasmonic core-satellite assembly. Guichi Zhu *et al* [115] have used a quencher-free fluorescent method for homogeneous sensitive detection of let-7a in human lung tissues. A method of Tungsten Disulfide (WS_2) nanosheet-mediated fluorescence quenching and duplex-specific nuclease signal amplification was adopted by Qiang Xi *et al* [116] for miR-21 detection. Partha Pratim [117] successfully developed a platform for fast detection of let-7 microRNA using polyaniline fluorescence and image analysis techniques. A real-time PCR method was adopted by Hong-He Zhang *et al* [118] for detection of let-7a in gastric carcinoma.

SPs were employed in this research work due to their excellent signaling property. It must also be stated that the aim of this work is to develop new smart probes (SPs) and homogeneous assays and to demonstrate their suitability for in vitro (and possibly, in vivo), sequence-specific detection of miR-21 and let-7a target sequences. However, these studies also show the inherent sensitivity of SP and demonstrate that this method can accurately recognize even single-base mismatches. It is expected that this work will build research competence in analytical method development and also represent a simple, fast and potential diagnostic tool for the various human cancers caused by miR-21 and let-7a.

2.5 How Smart Probes Work

Smart probes (SPs) are single-stranded nucleic acid molecules that possess a stem-and-loop structure (Fig 2.1). The ends of the probe contain a fluorophore and guanine base molecules. The loop portion of the molecule is complementary to the target sequences. The arm sequences are unrelated to the target sequence. A fluorophore is attached to one arm and multiple guanosine residues are attached to the end of the other arm. The close proximity of the guanosine residue and fluorophore causes the quenching of the fluorescence emission of the fluorophore. As shown in Figure 2.1, in the absence of target, the stems would hybridize with each other due to their close proximity and the SPs would form a hairpin structure. This would bring the dye very close to the guanine bases and induce dye-guanine interaction, which causes a significant reduction in the fluorescence of the dye. When the SPs encounter target sequences, SPs hybridize to their specific target sequence causing the hairpin-loop structure to open and separate the fluorophore from guanosine residues; it forms a hybrid that is longer and more stable than the hybrid formed by the arm sequences. Since nucleic acid double helices are rigid [105], the formation of SP-target hybrid rules out the simultaneous existence of a hybrid formed by the arm sequences. Since the fluorophore is no longer in close proximity to the guanine residues, fluorescence emission takes place. The measured signal is directly proportional to the amount of the target.

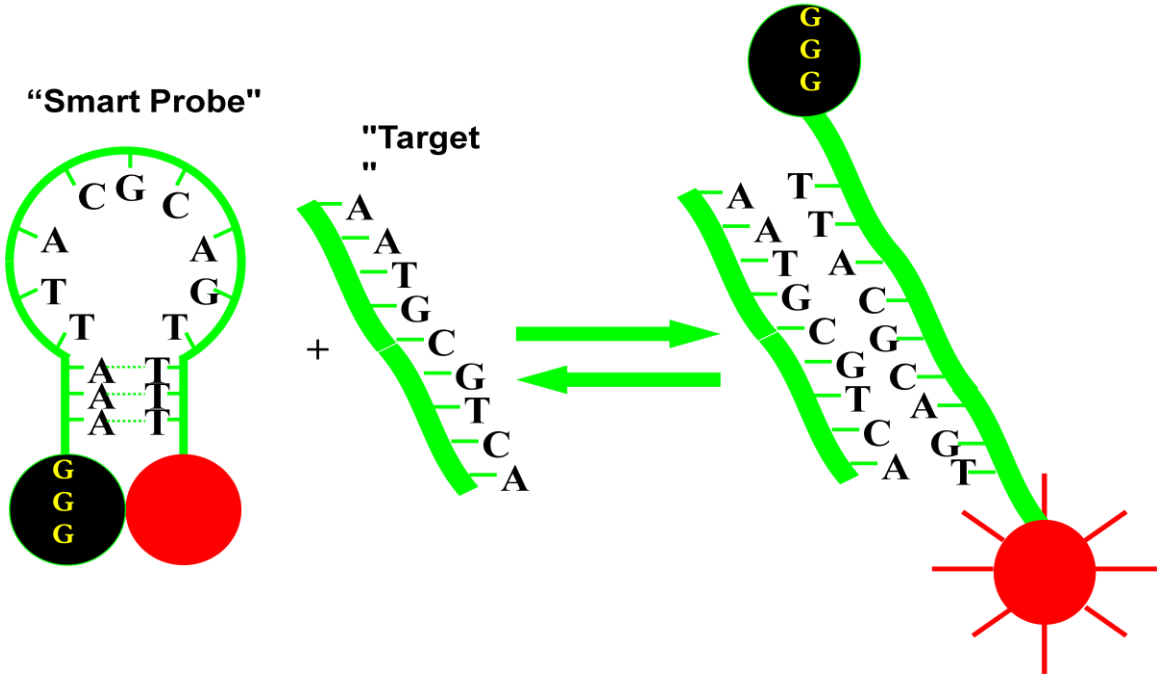

Figure 2.1: How Smart probes Work

CHAPTER 3

EXPERIMENTALS

3.1 Introduction

This chapter explains experimental details related to Smart Probes (SPs) characterization both in the presence and absence of the target sequence. The concept and experimental techniques of the various characterization methods used are concisely explained.

3.2 Materials and Reagent

Two smart probes and their corresponding oligonucleotide target sequences used in this study were custom synthesized and purified by Integrated DNA Technology, BVBA, Leuven, Belgium and are summarized in Table 3.1 and 3.2. All reagents were of analytical grade; sodium hydroxide (NaOH) (Fluka AG, Buchs, Switzerland), sodium chloride and magnesium chloride hexahydrate ($MgCl_2.6H_2O$) were purchased from (Fisher Scientific Company, New Jersey, NJ, USA) and (BDH Chemical Ltd. Poole, England) respectively. Hydrochloric acid and ethylenediaminetetraacetic acid (EDTA) were both obtained from BDH Chemical Ltd. (Poole, England). Tris was purchased from Sigma-Aldrich, (St. Louis, MO, USA). All chemicals were used as received. Nanopure water from a water purification system (Thermo Science, Waltham, MA, USA) was used for all solutions. Oligonucleotide samples and smart probe (SP) were each suspended in

nanopure water and were separated in aliquots and kept frozen at -20 ^{o}C until needed. After thawing, miR-21 was diluted in buffer (20 mM Tris, 2 mM EDTA, pH 7.5) in the presence of 200 mM NaCl and 3 mM $MgCl_2$, while let-7 was diluted in buffer (20 mM Tris, 2 mM EDTA, pH 7.5) in the presence of 200 mM NaCl and 20 mM $MgCl_2$ to gives desired concentration. The concentration of diluted oligonucleotide solutions were confirmed by using UV-Visible spectrophotometer (Genesys 10S UV-Vis spectrophotometer, Thermo Scientific, Waltham, MA, USA).

Table 3.1: List of oligonucleotide sequences for miR-21.

Name	Sequence
Smart Probe (SP)[a]	5'-/56-FAM/**<u>TCCCGAGG</u>**TCAACATCAGTCTGATAAGCTA**<u>CCTCGGGA</u>GGG**-3'
miR-21 target sequence (RNA1)[b]	5'-rUrArGrCrUrUrArUrCrArGrArCrUrGrArUrGrUrUrGrA-3'
miR-21 mismatch target sequence (RNA2)[b,c]	5'-rUrArGrCrUrUrArUrCrA**<u>rC</u>**rArCrUrGrArUrGrUrUrGrA-3'
miR-21 mismatch target sequence (RNA2b)[b,c]	5'-rUrArGrCrUrUrArUrCrArGrArCrUrGrArU**<u>rC</u>**rUrUrGrA-3'
miR-21 mismatch target sequence (RNA3)[d]	5'-rUrArGrCrUrU**<u>rG</u>**rUrCrArGrArCrU**<u>rA</u>**rArUrGrUrUrGrA-3'
miR-21 mismatch target sequence (RNA4)[b,c]	5'-rUrArGrCrUrUrArUrCrA**<u>rU</u>**rArCrUrGrArUrGrUrUrGrA-3'

[a]The underlined bases indicate the stem sequences, while the three G's on the 3' end is not part of the stem hybrid but are included as quenchers for the fluorophore.

[b]The underlined bases in RNA2, RNA2b and RNA4 is the single-base mismatch, whereby the corresponding rG in RNA1 has been replaced by rC in RNA2 and RNA2b and by rU in RNA4.

[c]The difference between RNA2 and RNA2b as compared to the RNA4 is in the location and type of the single-base mismatch.

[d]The underlined bases in RNA3 is the double-bases mismatch, whereby the corresponding rA and rG have been replaced by rG and rA respectively.

Table 3.2: List of oligonucleotide sequences for Let-7.

Name	Sequence
Smart Probe (SP)[a]	5'-/56-FAM/**<u>ACCCGG</u>**AACTATACAACCTACTACCTCA**<u>CCGGGTG</u>GG**-3'
Let-7a target sequence[b)]	5'-rUrGrArGrGrUrArGrUrArGrGrUrUrGrUrArUrArGrUrU-3'
Let-7b mismatch target sequence[b,c)]	5'-rUrGrArGrGrUrArGrUrArGrGrUrUrGrUr**<u>G</u>**rUr**<u>G</u>**rGrUrU-3'
Let-7c mismatch target sequence[b,c)]	5'-rUrGrArGrGrUrArGrUrArGrGrUrUrGrUrArUr**<u>G</u>**rGrUrU-3'
Let-7b mismatch target sequence blocker	AACCACACAACCTACTACCTCA
Let-7c mismatch target sequence blocker	AACCATACAACCTACTACCTCA

[a]The underlined bases indicate the stem sequences, while the three G's on the 3' end is not part of the stem hybrid but are included as quenchers for the fluorophore.

[b]The underlined bases in Let-7b and let-7c are double-bases and single-base mismatch, respectively, whereby the corresponding rA in Let-7a has been replaced by rG in Let-7b and let-7c.

[c]The difference between let-7b and let-7c is the number of base mismatch.

3.3 Fluorescence Measurements

The picture of a typical fluorescence spectrophotometer measurement setup is depicted in Fig 3.1. In brief, xenon lamp was employed as the excitation source. Fluorescence emission spectra were recorded in the range from 500 and 650 nm at an excitation wavelength of 490 nm. The emission wavelength of 520 nm was used for data analysis. The excitation and emission slits were set to 3.0 and 3.0 nm, except for calibration data,

where they were both set to 5.0 nm. A 10-mm path, sub-micro quartz cuvette was used for these measurements. A thermo-electrically cooled sample holder inserted in the fluorescence spectrophotometer regulated sample temperatures and TC125 temperature control unit (Quantum Northwest Inc., USA) was employed for changing the temperatures. For all the miR-21 thermal transition profile fluorescence measurements, 100 nM SP was mixed with 300 nM target (1:3 molar ratios in Tris-EDTA buffer). These solutions were then incubated in the dark at room temperature for about 5 hours prior to fluorescence measurements.

Figure 3.1: Picture of FLS 920 fluorescence spectrometer setup.

Fluorescence spectra of the incubated samples were measured using FLS920 fluorescence spectrophotometer. The spectra were recorded at room temperature on a 400 μL aliquot of the SP-oligonucleotide hybridization mixture. The temperature-dependent fluorescence measurements were carried out on buffer solutions of the SPs incubated in the presence or absence of the target oligonucleotide sequences. The temperature was varied from 20 to 78 ^{o}C in 2 ^{o}C increment, with 100 seconds settling time. For fluorescence measurements involving Let-7 SP in the presence of perfect target sequence, 100 nM SP was mixed with the 300 nM target (1:3 molar ratios in Tris-EDTA buffer). The experiments were repeated with imperfect targets that include single and double bases

mismatch, both in the absence of and in the presence of mismatch sequence blockers. These experiments were performed with individual mismatch sequences on the one hand, and all three targets (let-7a, let-7b and let-7c) as a mixture on the other hand, in the presence of blockers. For the individual mismatch targets, 50nM SP was mixed with 150nM mismatch sequence in the presence of 300nM mismatch sequence blockers (1:3:6 molar ratios in Tris-EDTA buffer).

For fluorescence measurement involving all three target in the absence of mismatch sequence blockers, 150 nM SP was mixed with 150 nM each of the three targets (let-7a, let-7b, and let-7c) respectively (1:1:1:1 molar ratio in Tris-EDTA buffer). Also, for fluorescence measurements performed in the presence of blockers, 150 nM SP was mixed with 300 nM excess of two mismatch blockers (let-7b and let-7c), in the presence of 150 nM of all the three targets (let-7a, let-7b, and let-7c) respectively.

The SP-Let-7a concentration-dependent experiment used 100 nM SP in the presence of varying concentrations of target oligonucleotide sequence (0-1000 nM) and incubated in the dark at room temperature for around five hours prior to fluorescence measurements.

For hybridization kinetic fluorescence measurements at room temperature, 100 nM SP was mixed with 300 nM target oligonucleotide sequence (1:3 molar ratios in Tris-EDTA buffer) in a reaction volume of 400 μL. Fluorescence intensity was measured at specified time intervals, immediately after mixing of an oligonucleotide with SP. Meanwhile, for kinetic experiments at 37 ^{o}C, fluorescence spectra were measured at specified time intervals, immediately after the mixing of an oligonucleotide with SP that has been thermostated at 37 ^{o}C for several minutes.

CHAPTER 4

RESULTS AND DISCUSSION

4.1 Design of the Smart Probes for the detection of miR-21 target

MicroRNA detection is very important to the understanding of cancer prognosis and progression. In order to develop methods for miRNA detection, hairpin probes have been designed. Smart probes (SP) are hairpin-shaped oligonucleotide probe molecules with a fluorophore on one end and multiple guanine bases on the opposing end are used as quenchers. The SP was precisely designed to maximize its performance as a specific and selective probe. The SP contained 41 nucleic acids bases (see Table 3.1). As for the target and mismatch sequences, the sequence of miR-21 (herein called RNA1) is perfectly complementary to the loop of the SP, while three others (RNA2, RNA2b, and RNA4) have a single-base mismatch in the complementary loop sequences (underlined, Table 3.1). Also, sequence RNA3 have two-base mismatches with the loop of the probe (underlined, Table 3.1). The loop sequence of the SP contained a 22-nucleotide-long sequence that is perfectly complementary to the miR-21 target sequence (Fig 4.1). The stem hybrid comprises of 8 nucleobases on each side (Fig 4.1). The fluorophore dye, 6-FAM (6-carboxyfluorescein) is on the 5’ end, and the multiple guanosine bases are on the 3’ end. To optimize the quenching by the guanosine residues, three of which form part of the stem and complementary to the cytosine residue on the 5’ side of the stem and the

remaining three form an overhang to additionally improve the quenching efficiency [105].

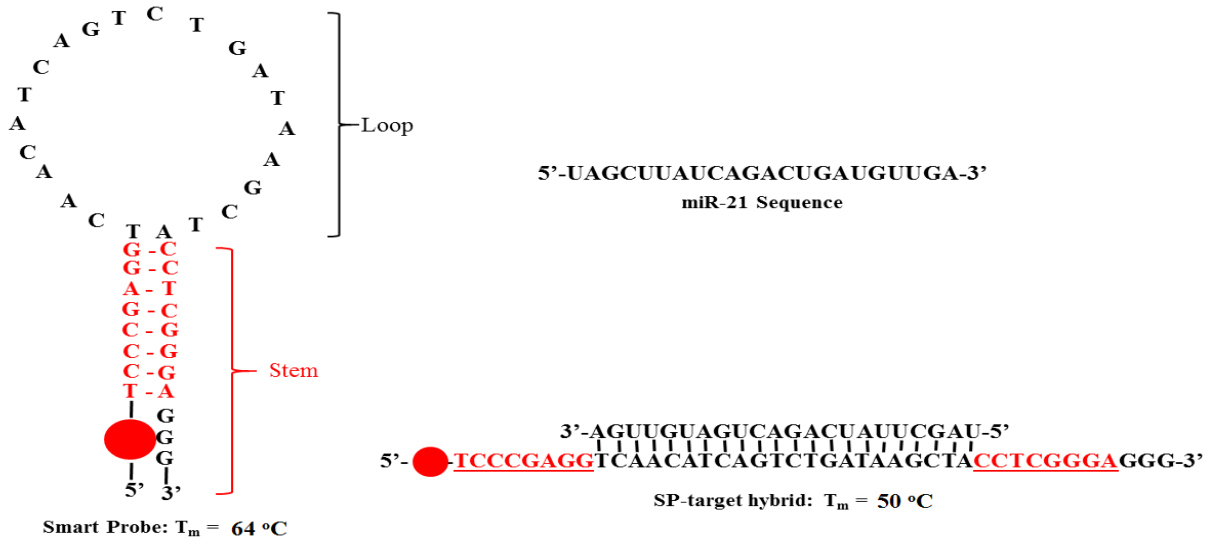

Figure 4.1: Structure of the SP and that of SP-RNA1 duplex and their T_m. The sequence of the miR-21 target is also shown (top right). setup.

The SP used in this thesis work was carefully designed to optimize its performance as a specific and sensitive probe for the miR-21 sequence. Since SPs have essentially the same properties and conformational structure as molecular beacons [MB], except for the absence of quencher component that is incorporated in molecular beacons, the factors affecting SP hybridization and their temperature-dependent conformation, such as melting temperature of the loop and the stem and target to probe concentration are similar to those of MB [119]. In light of the thermodynamic stability of MB, a functional MB or SP ought to have its stem more thermally stable than the SP-target duplex [109].

Optimization of the SP for sequence-specific detection was accomplished by ensuring that the stem melting temperature is sensibly higher than the SP-target hybrid melting temperature (T_m). This ensures that the stem remains intact as a hairpin at relatively high temperature when the SP-target hybrid has melted. These considerations have been factored in to ensure the correct design and performance of the SP. As shown in Fig 4.1, the T_m of the SP is 64 ^oC, while that of SP-RNA1 sequence hybrid is 50 ^oC. Thus, the T_m of SP-RNA1 hybrid is 14 ^oC lower than that of SP alone. Therefore, based on the hybrid T_m, these SP possesses excellent specificity and sensitivity.

4.2 Thermal Transition Profile

SPs should exhibit a conformational change upon heating that is consistent with their design. When the temperature of a solution containing SP is increased, fluorescence increases in a manner that is characteristic of the melting of the double-stranded nucleic acids [108]. To ensure correct design and optimal performance of the SP, thermal denaturation profiles of the SP alone and SP-RNA1/RNA2/RNA2b/RNA3/RNA4 duplexes were measured. Figure 4.2 shows the thermal transition profiles derived from the heating cycle for the SP and SP-target hybrids for the five oligonucleotide sequences.

In Fig. 4.2, the thermal transition profile of SP alone confirms that at low temperature the SP exists in the hairpin form, and the fluorescence of the fluorophore is quenched by the guanines residue on the 3' end (black, Figure 4.2). However, as the temperature is increased to about 58 ^oC, the stem hybrid begins to melt, and the fluorophore separates

from the guanine residues. When the temperature is further increased, the fluorophore and the guanine residue are separated further, until the stem hybrid completely melts.

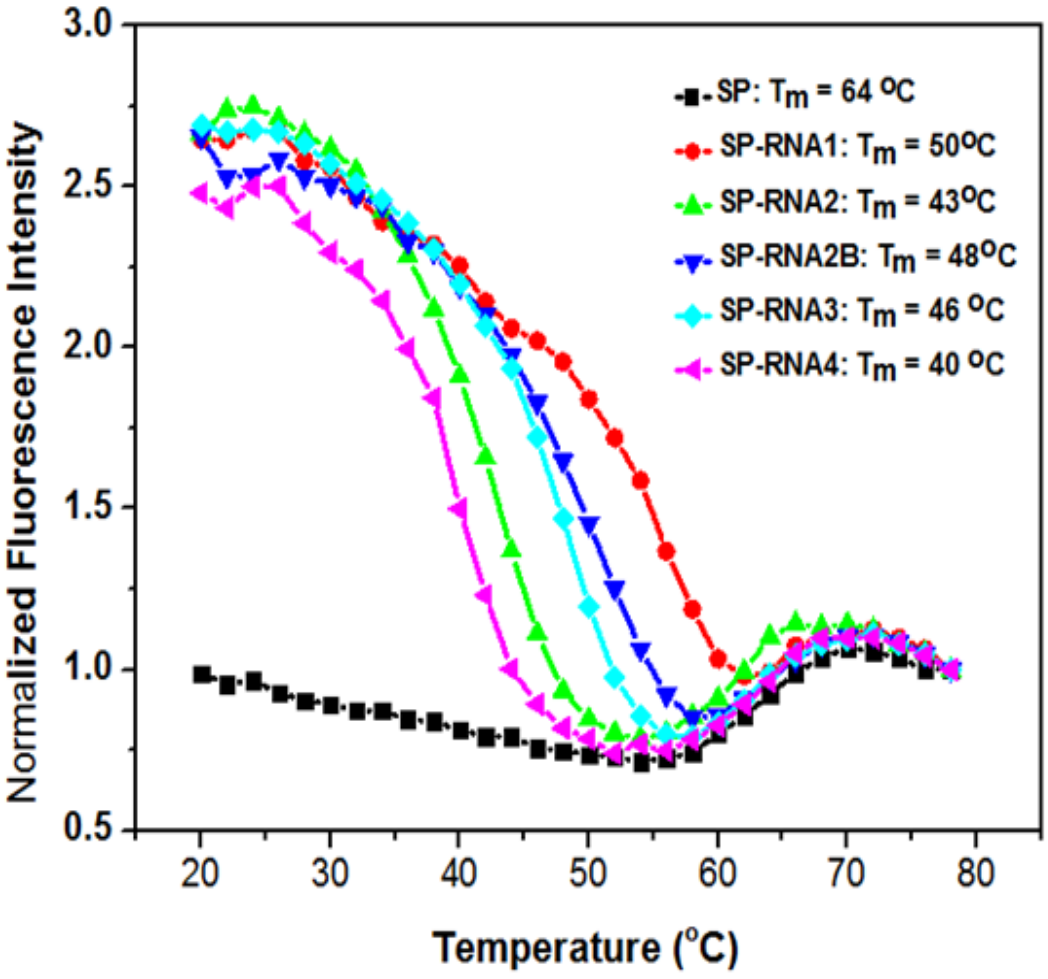

Figure 4.2: Thermal transition profiles of SP (black), SP-RNA1 (red), SP-RNA2 (green), SP-RNA2b (blue), SP-RNA3 (cyan) and SP-RNA4 (magenta) target sequences. Each measured fluorescence intensity has been normalized to the intensity at 78 °C.

This is evidenced by an increase in fluorescence intensity with increase in temperature between 58 and 70 ^{o}C. Beyond this point, the SP stem adopts a random-coil conformation and the fluorescence intensity goes down slightly.

In the presence of a three-fold excess of perfectly complementary miR-21 target sequence (RNA1), the fluorescence intensity was very high at low temperature (red, Figure 4.2), because the miR-21 target sequence hybridized with the loop sequence of the SP, resulting in the SP undergoing a spontaneous conformational change that forces the fluorophore and the quenching guanine residues apart. As the temperature was gradually raised further, fluorescence begins to decrease, which suggests the stable hybrid is gradually melting and the fluorophore and guanine quencher are moving closer, due to the SP forming a hairpin. This decrease continues with an increase in temperature until the RNA1 target completely melts away from the SP and the SP assumes the hairpin conformation, with the fluorophore in contact with the guanosine residues, which indicated the lowest point on the curve (red, Figure 4.2). As the temperature is further increased, the stem of the hairpin then gradually melts and the fluorescence intensity begins to increase again until the stem adopts a random-coil conformation and the fluorescence is decreases further. The T_m of SP-RNA1 was determined to be 50 ^{o}C and the difference in T_m between SP alone and SP-target duplex is 14 ^{o}C. This difference in T_m suggests excellent recognition of the RNA1 target sequences by the smart probes and specificity of the new SP developed. There is about a three-fold increase in fluorescence intensity at 20 ^{o}C when the fluorescence intensity of the SP alone is compared to the SP-RNA1 sequences. This intensity increase is consistent with that reported previously for SP [110].

A similar pattern is observed when there is single (green, blue, and magenta Figure 4.2) and double (cyan, Figure 4.2) base mismatches in the target sequences, with relatively low melting temperatures. The shape of the thermal transition profile is similar to that of SP-RNA1 (red, Figure 4.2) and the difference in T_m between SP alone and the SP-target duplex (21 ^oC for SP-RNA2 sequence, 16 ^oC for SP-RNA2b sequence, 18 ^oC for SP-RNA3 sequence and 24 ^oC for SP-RNA4 sequence) suggest the specificity of this new probe for preferentially detecting the target miR-21 sequence against the mismatch sequences.

4.3 Enhanced Temperature-Dependent Discrimination

Figure 4.2 suggests a number of ways for discriminating between the miR-21 target sequence, RNA1, and the mismatch sequences, RNA2, RNA2b, RNA3 and RNA4. This includes measurement of the thermal transition profiles to decide the T_m for each situation; and single-point estimation of the fluorescence intensity at a high temperature of around 56 ^oC. The ideal approach to discriminate between RNA1 and the four mismatches RNA2, RNA2b, and RNA3 and RNA4 duplexes is by measuring the fluorescence intensities of all five duplexes around 56 ^oC. Due to the fact that at this temperature, fluorescence intensity produced by each of SP-RNA2, SP-RNA2b, SP-RNA3 and SP-RNA4 sequence hybrid is significantly quenched, much like that of SP alone (Figure 4.2). Then again, SP-RNA1 target hybrid gives a substantially higher fluorescence signal at 56 ^oC. Hence, looking at the fluorescence signal at 56 ^oC for each of the five duplexes (SP-RNA1, SP-RNA2, SP-RNA2b, SP-RNA3 and SP-RNA4), the signal produced by RNA1 is around 165% that of SP-RNA2, SP-RNA2b, SP-RNA3 and

SP-RNA4 (Figure 4.3). This implies that at 56 ^{o}C, SP is hybridized with the RNA1 and accordingly fluoresces, while SP is not hybridized with RNA2, RNA2b, RNA3 and RNA4, resulting in a fluorescence signal that is quenched. In this way, by measuring the fluorescence signal at 56 ^{o}C, miR-21 target sequences can be specifically detected while the fluorescence signal from mismatch sequences is significantly quenched. Thus, this SP has shown the inherent sensitivity and demonstrated that this method can accurately recognize mismatched sequences.

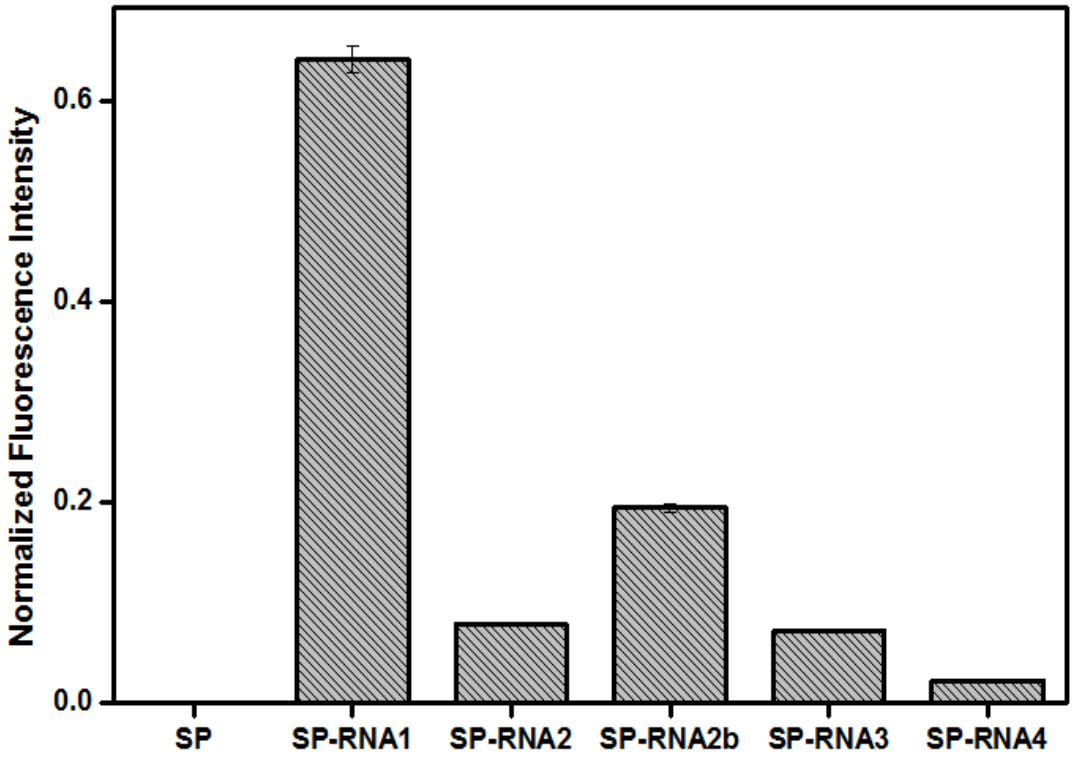

Figure 4.3: The miR-21 sequence discrimination at 56 ^{o}C. This data was extracted from thermal transition profile and the raw signal for SP alone was subtracted from those of SP-target signals.

4.4 Hybridization Kinetics Measurements

SPs hybridize spontaneously to their target at room temperature and undergo a conformational change that results in the generation of fluorescence. Hybridization process of the SP with miR-21 (RNA1) at room temperature took around five hours to complete (Figure 4.4). This SP-target hybridization kinetics is consistent with the previously reported hybridization involving SPs and MBs [108-109]. However, five hours is a fairly lengthy time-frame if this technique is to be adapted for quick diagnostic applications. Therefore, the time-dependent investigation was performed at 37 ^{o}C, so as to accelerate the SP-target sequence hybridization and to be consistent with body temperature (see Figure 4.5). As shown in this Figure, complete hybridization process at 37 ^{o}C took just 40 minutes. This figure indicates that the hybridization process was so fast that the reaction was completed in 40 minutes for SP-target sequence, which is around seven times speedier than room temperature. Thus, the hybridization process can be completed in a really short time if the SP is hybridized with miR-21 at 37 ^{o}C.

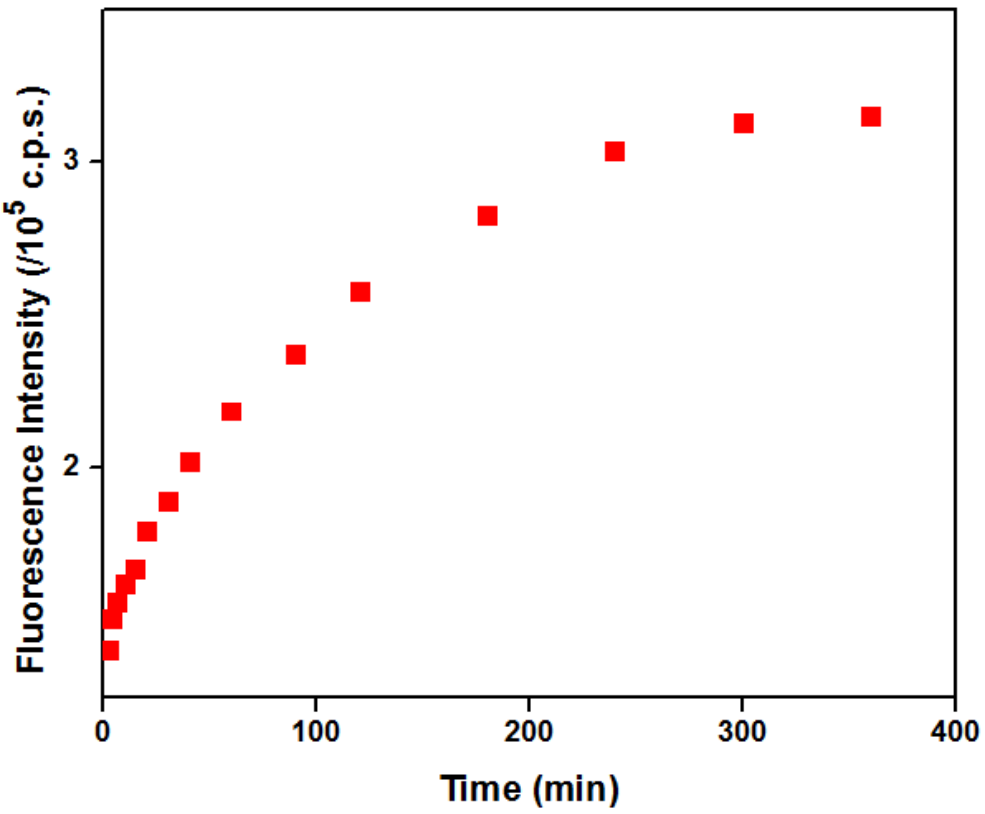

Figure 4.4: Time-dependent fluorescence signal of SP-RNA1 incubated at 22.5 ^{o}C

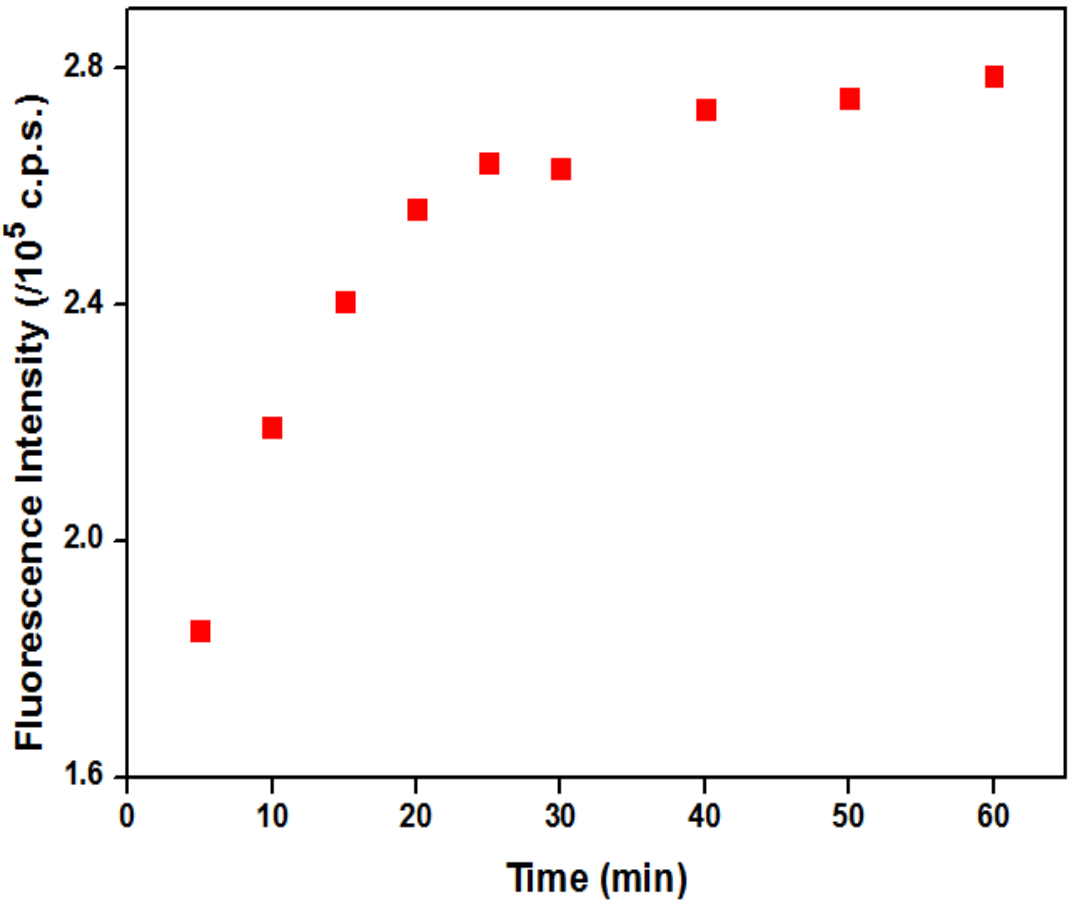

Figure 4.5: Time-dependent fluorescence signal of SP-RNA1 incubated at 37 ^{o}C.

4.5 Concentration-Dependent Measurements

To demonstrate the performance of this SP-based assay, concentration-dependent measurements were carried out. Different concentrations (0 to 1000 nM) of RNA1 was incubated with 100 nM SP for about 5 hours, followed by fluorescence intensity measurements. The fluorescence intensity of RNA1 increased with the increasing RNA1 concentration until RNA1 concentration of 100 nM. Thus, the calibration plot is linear in the 0-100 nM RNA1 concentration range (Figure 4.6), and the curve becomes nonlinear beyond 100 nM RNA1 target concentration (Figure 4.6 and 4.7). As shown in Figure 4.6, the detection limit of 0.53 nM (LOD = $3\sigma_{b1}/m$) was achieved. The limit of quantitation was found to be 1.76 nM (LOQ = $10\sigma_{b1}/m$), where σ_{b1} is the standard error of 3 replicate measurements of the blank (100 nM SP) and m is the slope of the calibration plot (Figure 4.6). The sensitivity of 14.0×10^{11} c.p.s.M^{-1} (Sensitivity = slope of the calibration plot) was achieved. These results are consistent with those already reported for SP and MB [99, 120].

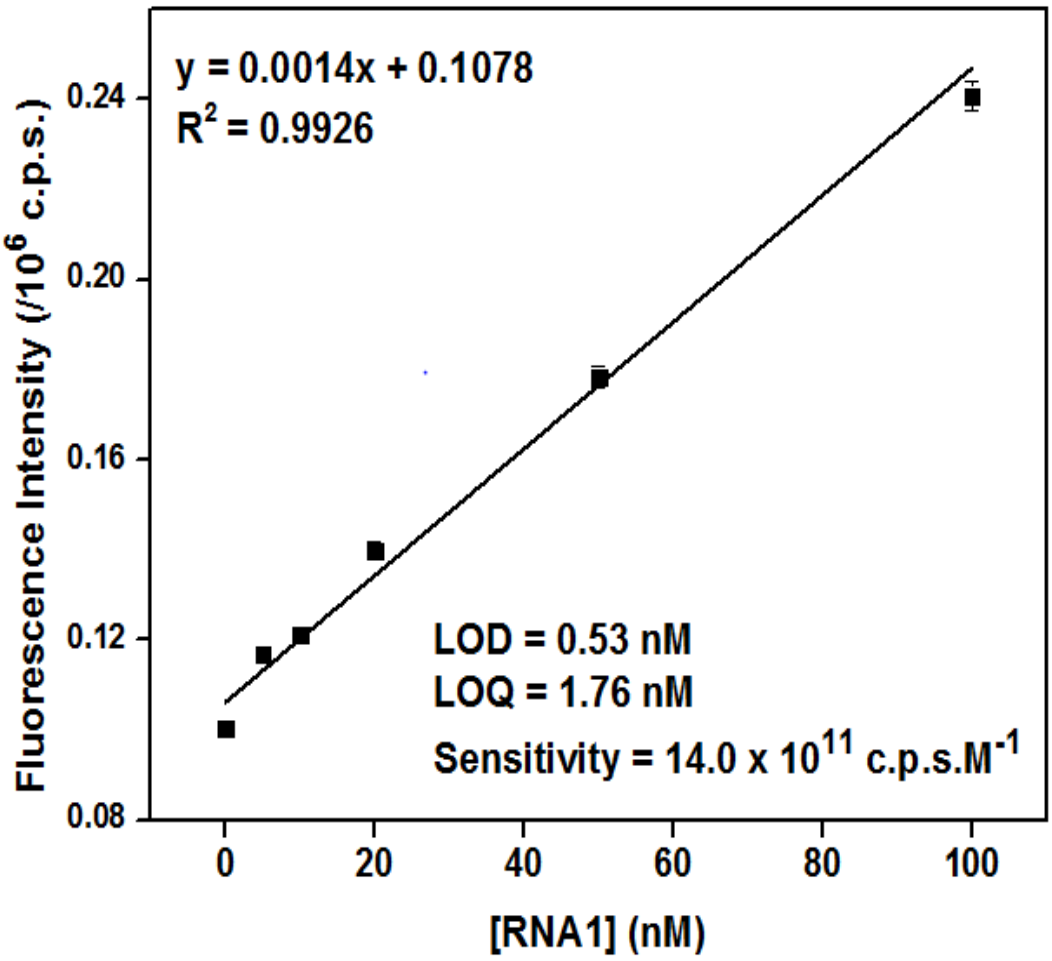

Figure 4.6: Linear portion of the Calibration plot for the detection of miR-21 sequence.

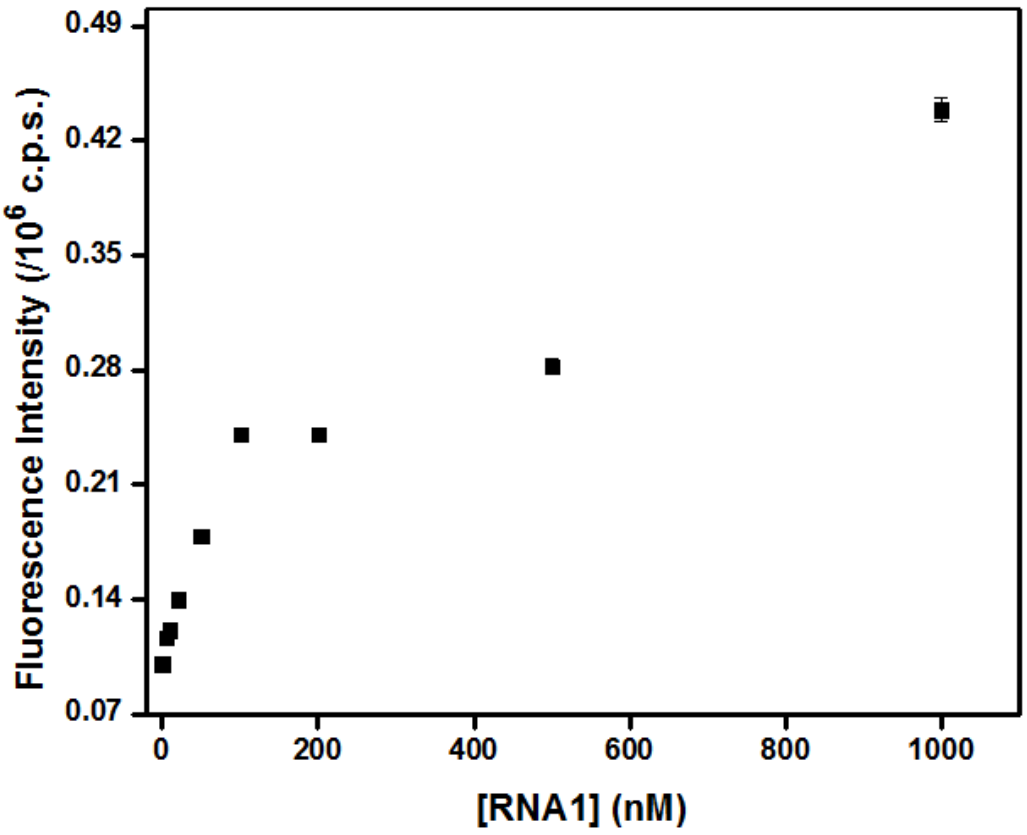

Figure 4.7: Concentration-dependent plot for 100 nM SP in the presence of different concentrations of RNA1 (0-1000 nM). Curve becomes non-linear beyond 100 nM RNA1 target concentration.

CHAPTER 5

Detection of Let-7a Cancer Biomarker Using a Smart Probe

5.1 Design of a Smart Probes for the detection of Let 7 target

The design principle of the new proposed smart probe (SP) is illustrated in Figure 5.1. The SP consists of a total of 37 nucleic acids bases, while the target sequences are the perfect sequence of Let-7a, and its corresponding double-base and single base mismatch sequence (Let-7b and Let-7c) respectively (see Table 3.2). The SP was synthesized with a 22-nucleotide loop that is complementary to this target sequence and a stem composed of 6 nucleobases on each side (Figure 5.1). The SP was labeled with a 6-FAM fluorophore on the 5'-end of the stem and with a 3-G quencher on the 3' ends (Figure 5.1). In addition to the 3-G quencher, more G bases are incorporated in the stem to further enhance the quenching. The SP stem sequence is only involved in the hairpin formation, not in binding to the target sequences.

The SP was carefully designed to optimize its performance as a specific and sensitive probe for Let-7a sequence. Optimization of the SP for sequence-specific detection was accomplished by ensuring that the stem melting temperature is sensibly higher than the SP-target hybrid melting temperature (T_m). This ensures that the stem remains intact as a hairpin at relatively high temperature when the SP-target hybrid has melted. These considerations have been taken into account in ensuring the correct design and performance of the SP. As shown in Fig 5.1, the T_m of the SP is 58 ^oC, while that of SP-

Let 7a hybrid is 48 ^{o}C. Thus, the T_m of SP-Let 7a hybrid is 10 ^{o}C lower than that of SP alone. Therefore, based on the hybrid T_m, the desired performance characteristic on the SP has been met.

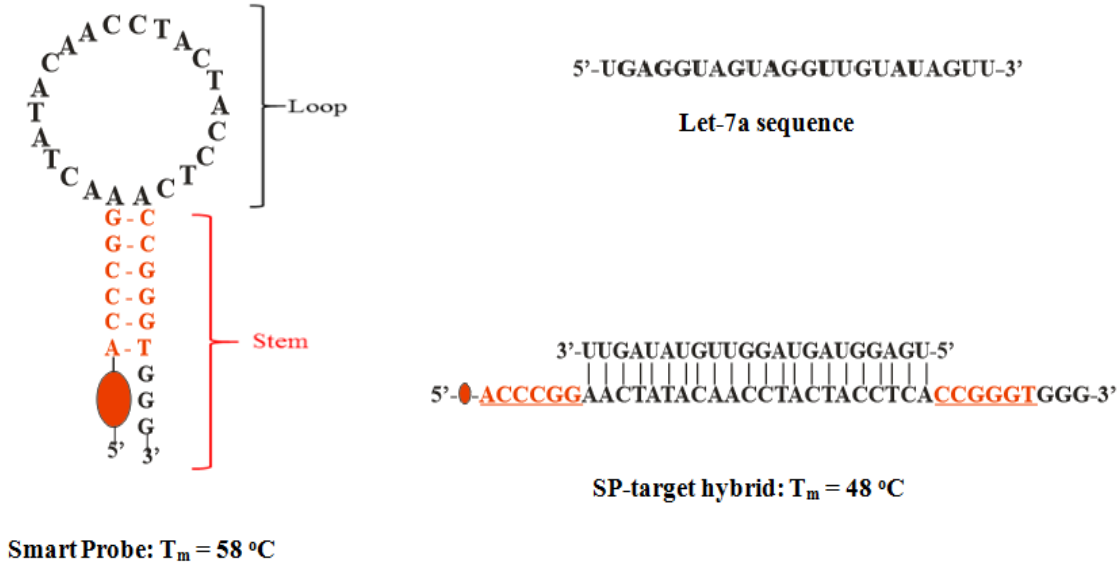

Figure 5.1: Structure of the SP and that of SP-Let 7a hybrid and their melting temperatures. The stem sequences of the SP are underlined in the SP-Let 7a hybrid (bottom right) for easy correlation with the structure of the SP on the left. The Let-7a target sequence is also shown (top right).

5.2 Thermal Transition Profiles

To ensure the correct design and performance characteristics of the new SP, thermal transition profile of the new SP was measured. Also, in order to ensure that SP can optimally recognize target oligonucleotide sequences, the SP stem must be closed and exhibit minimum fluorescence in the absence of target sequence, while in the presence of perfectly complementary target sequence, the SP must form a stable SP-target hybrid and exhibit maximum fluorescence. In addition, in the presence of mismatch sequences, the SP stem should somewhat keep the closed state, since the hybridization of the SP to the sequence that contains the mismatch form a less stable hybrid.

5.2.1 Thermal Transition Profile in the Absence of Blockers

In Fig 5.2 (black), the thermal transition profile of SP alone shows that at a lower temperature the SP still keeps the closed state, and the fluorescence is significantly quenched. However, as the temperature is increased, the stem hybrid begins to melt and the fluorophore and the quenching guanine residues move away from each other. When the temperature was further increased, the stem hybrid adopts a random-coil conformation and the fluorescence intensity goes down slightly. The T_m of the SP was determined to be 58 ^oC.

In the presence of a three-fold excess of Let-7a target sequence that was perfectly complementary to the loop sequence of the SP, the thermal melting curves are reverse,

that is, the fluorescence intensity is very high at low temperature, but the fluorescence decreases

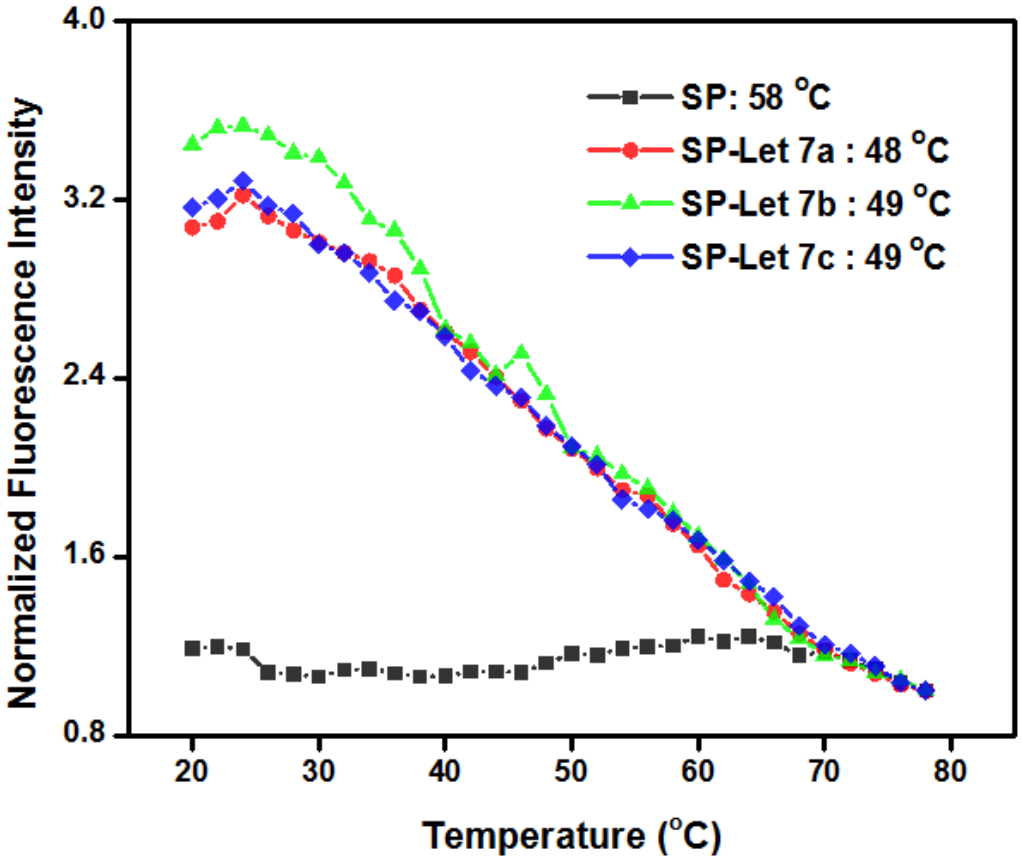

Figure 5.2: Thermal transition profiles of SP (black), SP-Let 7a (red), SP-Let7b (green) and SP-Let7c (blue), target sequences. Each measured fluorescence intensity has been normalized to the intensity at 78 °C.

significantly as the temperature is slowly increased. In the presence of Let-7a target, the highly fluorescent SP-Let 7a duplex hybrid forms spontaneously at low temperature. As the temperature is increased, the SP-Let 7a duplex becomes destabilized, the SP separates fully from the Let-7a target and forms its hairpin structure and the fluorescence is quenched (red, Figure 5.2). T_m of the SP-Let7a hybrid was determined to be 48 ^oC (red, Figure 5.2).

A similar pattern is observed when there is single (blue, Figure 5.2) and double (green, Figure 5.2) base mismatches in the target sequences. The shape of the thermal transition profile is similar to that of SP-Let 7a (red, Figure 5.2) and the differences in T_m between SP and the SP-target duplex (9 ^oC for SP-Let 7b and SP-Let 7c sequence respectively) suggest the specificity of this new probe for detecting the Let-7a sequence is poor. The results show that all three target sequences produce transition profile that are overlapping, so there is no difference between let-7a, let-7b, and let-7c target sequence because the sequences are so similar. These results are consistent with what was predicted for the T_m of the hybrid of SP with each of let-7a, let-7b and let-7 by OligoAnalyzer, a software used to predict melting behavior and T_m of oligonucleotide probes and their target hybrids. Let-7a, let-7b and let-7c all have essentially the same T_m under similar conditions. While this observation is a disadvantage, it in fact suggests that this new SP can in fact be used as a universal probe for Let-7a, let-7b and let-7c sequences. In order to enhance the specificity of the SP for let-7a and discriminate this target from the mismatch sequences of let-7b and let-7c, we use nucleic acid blockers. The nucleic acid blockers are unlabeled and perfectly complementary to mismatch sequences so that they can preferentially hybridized with such mismatch sequences, thereby preventing the SP

from hybridizing with such mismatch sequences (see Table 3.2). So, if this new SP is to be used for one target, we have to add blockers for other two targets. Therefore, instead of designing a different probe for the three let-7 targets, one can make use of this same probe for all the three targets.

5.2.2 Thermal Transition Profile in the Presence of Blockers

When the SP was mixed with a six-fold excess of Let-7b blockers sequence, and then followed by a three-fold excess of double-base mismatch sequence (Let-7b), the fluorescence intensity for SP-Let-7b hybrid is very low at low temperature (green, Figure 5.3). This is because the hybridization of the fluorescent SP to the Let-7b sequence containing the mismatch is blocked by the nucleic acid blockers and consequently no significant increase in fluorescence is found, so the SP is in the closed state. The let-7b blockers is perfectly complementary to Let-7b sequence. Also, the blockers are linear oligonucleotides and so have no stem-loop structure (see Table 3.2). However, as the temperature is increased, the stem hybrid of the SP begins to melt and the fluorophore and the guanine residues move away from each other. When the temperature was further increased, the stem hybrid adopts a random-coil conformation, in which case the fluorescence intensity go down slightly. For this profile, the T_m of the SP-Let7b hybrid in the presence of let-7b blockers was determined to be 57 ^{o}C (green, Figure 5.3). The T_m is essentially the same as that of SP, showing that the SP does not hybridize with Let-7b.When the SP was mixed with a six-fold excess of Let-7c blockers sequence in the presence of a three-fold excess of single-base mismatch sequence (Let-7c), low-intensity

signal was obtained at low temperature with a thermal profile similar to that of SP (blue, Figure 5.3) and a T_m of 57 ^oC.

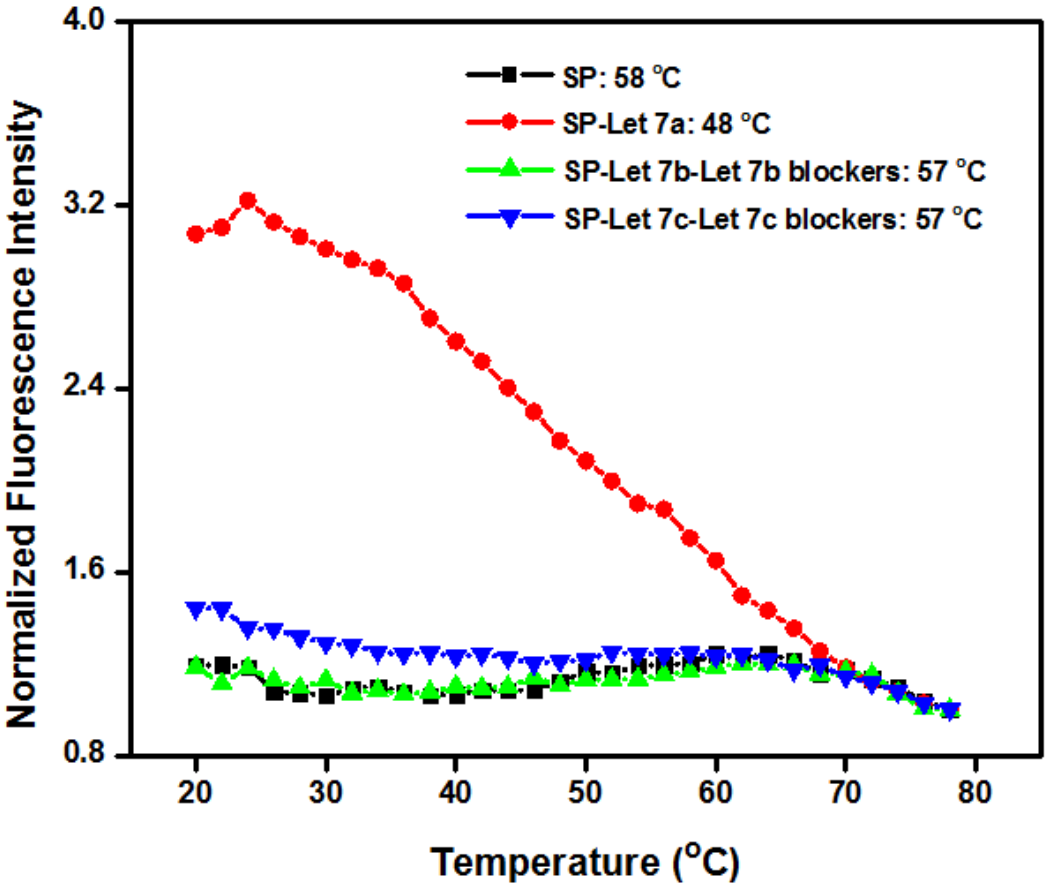

Figure 5.3: Thermal transition profiles of SP (black), SP-Let 7a (red), SP-Let7b in the presence of let-7b blockers (green) and SP-Let7c hybrid in the presence of let-7c blockers (blue). Each measured fluorescence intensity has been normalized to the intensity at 78 ^oC. Each of these four curves represent a separate experiment.

When the SP was mixed with a six-fold excess of the two blocking oligonucleotides (Let-7b and let-7c blockers) in the presence of a perfectly complementary Let-7a target sequence (Let-7a) and each of the two mismatches target sequences (Let-7b and let-7c sequences), the fluorescence intensity is very high at low temperature (blue, Figure 5.4). This is because the perfectly matched target sequence let-7a hybridized with the loop of the SP, and the fluorescence signal is recovered because the unfolding of SP increase the spatial distance of fluorophore and quenching guanine residues whereas the mixture of the mismatched sequences is effectively blocked by let-7b and 7c blockers. When the perfectly matched target sequence and the mismatched sequences are simultaneously present, the SP appeared to have hybridized with the perfect target sequence and the mismatched sequences, hence the observed approximately 15% decrease in fluorescence signal around 20 ^{o}C when compared to the mixture of the perfect and mismatched target sequences in the presence of let-7b and 7c blockers (green, Figure 5.4). This is because the SP appears to be competing with all the targets: perfect sequence let-7a and the mismatch sequences Let-7b and Let-7c, which may have brought down the intensity a little bit when 7b and 7c blockers were not present. The shape of the thermal transition profile for SP alone (black, Figure 5.4) and SP-target hybrid (red, Figure 5.4) are similar to those found for SP alone and SP-target hybrid in above reports (Figure 5.2). Thus, it is noteworthy that this method shows excellent specificity and sensitivity of the new SP using nucleic acid blockers and it enables efficient discrimination between perfect target sequences from analogous mismatch sequences.

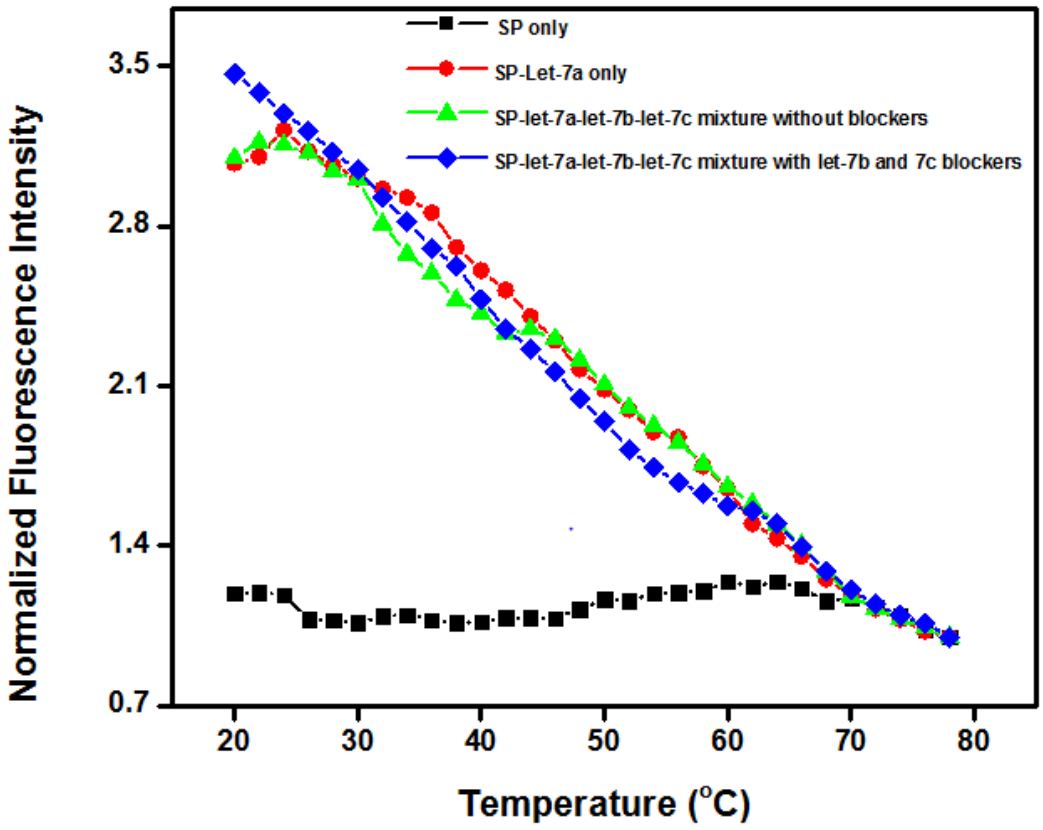

Figure 5.4: Thermal transition profiles of SP (black), SP-Let7a (red), SP-Let7a-let7b-let7c without blockers (green), and SP-Let7a-let7b-let7c in the presence of let-7b and 7c blockers (blue). Each measured fluorescence intensity has been normalized to the intensity at 78 °C. This is a single-pot experiment where SP-Let-7a, was measured in the presence of let-7b and let-7c and their corresponding blockers.

5.3 Enhanced Temperature-Dependent Measurements

Figure 5.3 suggest possible ways of discriminating between the target sequence, Let-7a and its analogous mismatch sequences (Let-7b and Let-7c). This includes: measuring the thermal denaturation profile to determine the melting temperature in each case and single-point measurement of the fluorescence signal of all the three duplexes at 20 ^{o}C. This is because the fluorescence intensity produced by SP-Let 7a at this temperature is very high whereas the fluorescence signal produced by SP-Let 7b and SP-Let 7c duplexes is quenched in the presence of blockers, just like that of SP alone (Figure 5.3). Thus when fluorescence intensity was measured at 20 ^{o}C for all the three duplexes (SP-Let 7a, SP-Let 7b and SP-Let 7c), the intensity produced by SP-Let 7a hybrid is around 180% that of SP-Let 7b and SP-Let 7c (Figure 5.5). Hence, at 20 ^{o}C, the SP is hybridized with Let-7a whereas the hybridization of the SP to the sequences containing mismatches (Let-7b and Let-7c) is prevented by the nucleic acid blockers and therefore produced fluorescence intensity that is significantly quenched. Thus, it can be clearly seen that the use of these nucleic acid blockers significantly enhances the sequence-specificity of the SP.

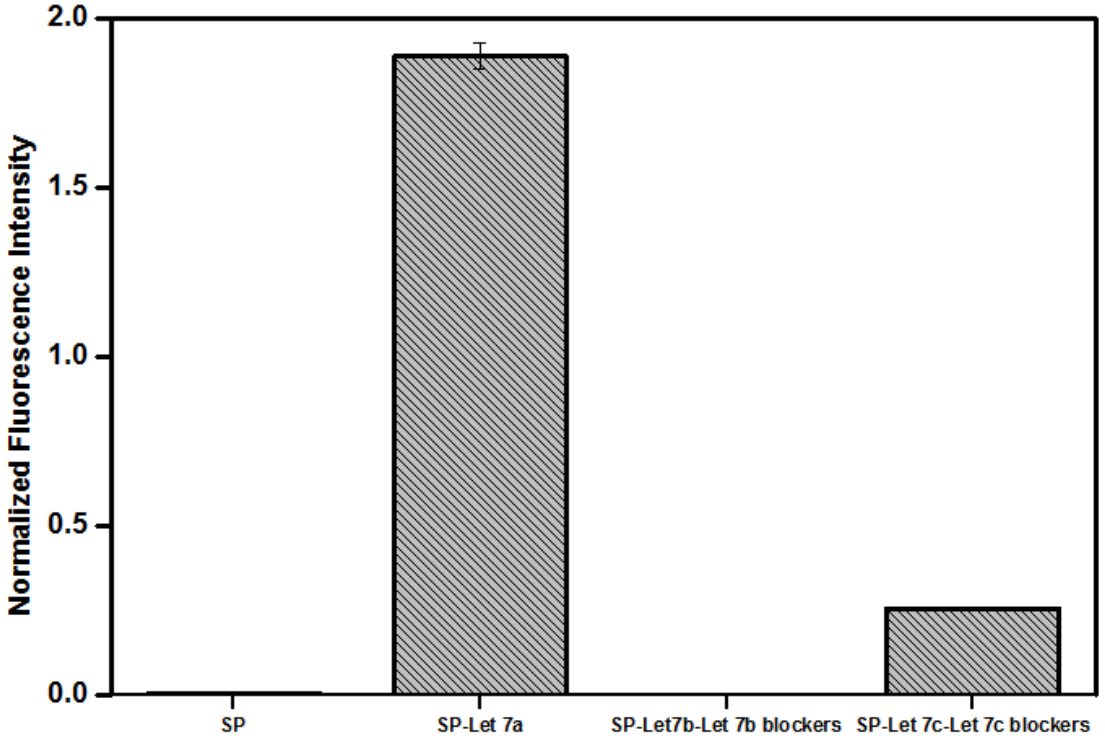

Figure 5.5: The Let-7 sequence discrimination at 20 ^{o}C. This data was extracted from thermal transition profiles (Figure 5.3).

5.4 Concentration-Dependent Measurements

In order to determine the sensitivity and performance of the SP assays, concentration-dependent measurements were carried out. Different concentrations (0 to 1000 nM) of Let-7a were hybridized with 100 nM SP and then followed by fluorescence intensity measurements. The fluorescence intensity of SP-Let-7a hybrid increased with increasing Let-7a concentration until 200 nM. The calibration curve is linear in the 0-5 nM Let-7a concentration range (Figure 5.6), and the curve becomes nonlinear beyond 5 nM Let-7a target concentration (Figure 5.6 and 5.7). As shown in Figure 5.6, the detection limit of

0.02 nM (LOD = $3\sigma_{b1}/m$) was achieved. The limit of quantitation was found to be 0.07 nM (LOQ = $10\sigma_{b1}/m$), where σ_{b1} is the standard error of 3 replicate measurements of the blank (100 nM SP) and m is the slope of the calibration plot (Figure 5.6). The sensitivity represents the slope of the curve and was found to be 44.2 x 10^{12} c.p.s.M^{-1}.

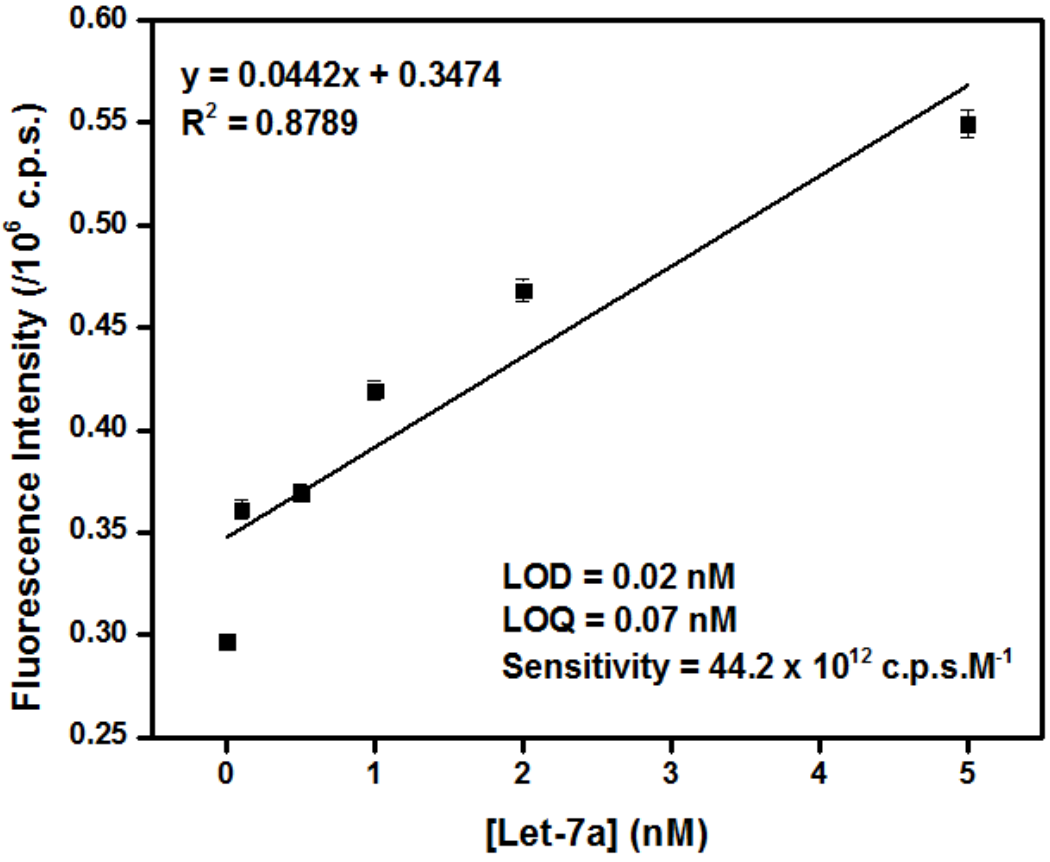

Figure 5.6: Linear portion of the Calibration plot for the detection of Let-7a sequences.

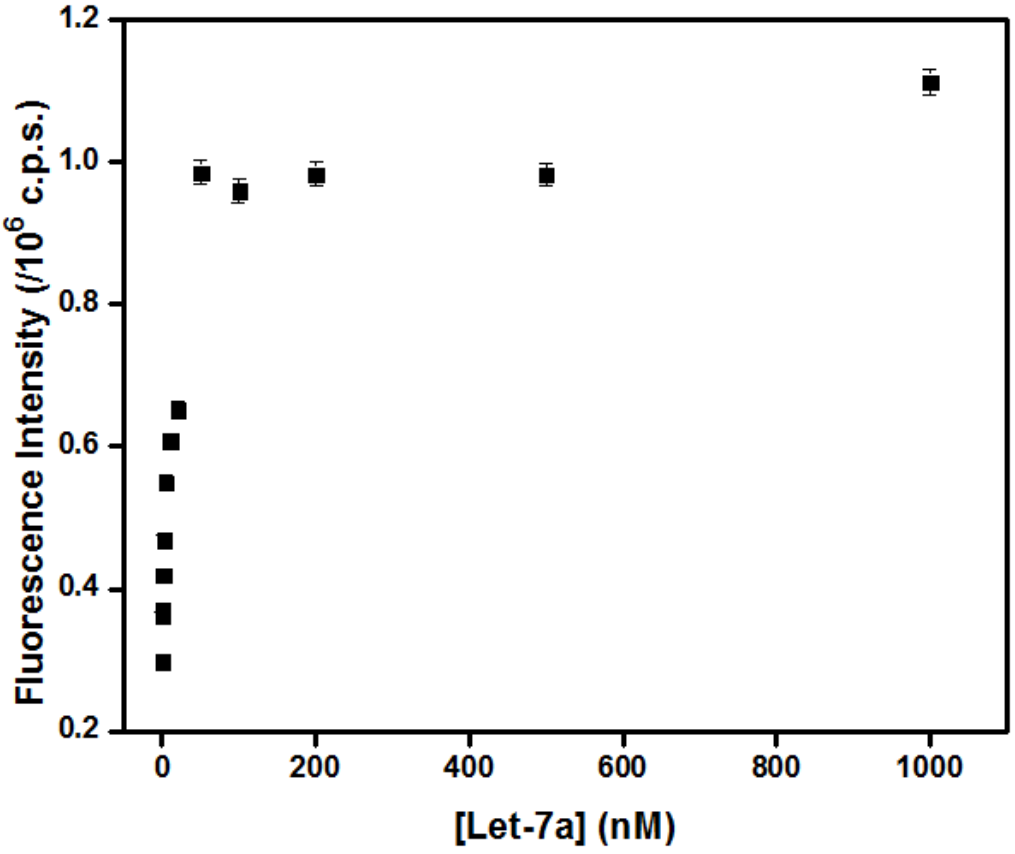

Figure 5.7: Concentration-dependent plot of 100 nM SP in the presence of different concentrations of Let-7a (0-1000 nM). Curve becomes non-linear beyond 5 nM Let-7a target concentration.

5.5 Comparison of the Developed Method to Prior Methods

Comparing the SP-based method developed in this work to the methods outlined in the introduction, the method is quite simple and specific, with the detection limit in nanomolar concentration range. This technique is like PCR based techniques in term of sensitivity. On the basis of simplicity and cost, the SP-based method is an improvement over the PCR detection method because PCR is time-consuming and costly [104].

The northern blot method presents low sensitivity than the method presented in this work, it is complex and requires radiolabeling [87-90], while this new method is less cumbersome and simpler. Also, the high cost of fluorescence quencher-based techniques makes their potential use for multiplex analysis of a large number of different specific target sequences difficult and unattractive [35]. Also, this SP method is very fast, taking 40 minutes to detect target if the SP and target were incubated at 37 ^{o}C This SP-based method gives nanomolar sensitivity. Thus, this SP-based method is quite simple, enzyme-free and rapid, and it provides high specificity for the target sequence. It is notable that the technique presented here shows excellent specificity since we apply nucleic acid blockers that hybridized to the Let 7 sequences containing base mismatches.

CHAPTER 6

CONCLUSION

In this work, we have successfully designed and characterized two new SPs for highly specific detection of miRNA in a homogenous assay format. Each SP consists of a dye-labeled stem-loop structure that undergoes conformational change upon specific hybridization to the target sequence. The loop sequence of each SP is perfectly complementary to the miRNA sequence of interest. The thermal transition of each SP shows that the SP can give a fluorescence intensity increase of about three-fold when it is bound to a perfectly complementary target. Our result shows that each SP has excellent sensitivity and specificity which make it suitable to discriminate between perfect targets and mismatch target sequences. It was additionally discovered that recognition of miRNA target with the SP finished in around 40 minutes if the two components were incubated at 37 ^{o}C. This SP-based method is very fast, simple, cheap and less cumbersome when contrasted with other methods reported for miRNA detection. Also, this SP gives nanomolar sensitivity. Compared with other miRNA detection methods, this method shows high sensitivity, improved mismatch discrimination and decreased cost due to high fluorescence quenching efficiency of the use of a single-label probe. Therefore, the simplicity, cheap cost and excellent specificity of the new SPs make them suitable tools for fast in vitro detection of miRNAs. The assay reported here gives a detection limit of (0.53 and 0.02 nM), a limit of quantitation of (1.76 and 0.07 nM) and a sensitivity of (14

x10^{11} and 44.2 x 10^{12} c.p.s.M^{-1}) for miR-21 and Let-7a respectively. The detection sensitivity reported here is in nanomolar concentration which is consistent with literature results for MB and SP-based methods. This new SP-based method does not involve any amplification steps. Therefore, the SP-based method presented here is fast, simple and specific, and represent a unique platform for homogenous assay analysis for miRNAs.

References

[1] T. T. M. Lagos-Quintana, R. Rauhut, W. Lendeckel, "Identification of Novel Genes Coding for Small Expression RNAs.," *Science (80-.).*, vol. 294, pp. 853–858, 2001.

[2] S. Zhu, M. L. Si, H. Wu, and Y. Y. Mo, "MicroRNA-21 targets the tumor suppressor gene tropomyosin 1 (TPM1)," *J. Biol. Chem.*, vol. 282, no. 19, pp. 14328–14336, 2007.

[3] G. A. Calin and C. M. Croce, "MicroRNA signatures in human cancers," *Nat. Rev. Cancer*, vol. 6, no. 11, pp. 857–866, 2006.

[4] Q. Huang *et al.*, "The microRNAs miR-373 and miR-520c promote tumour invasion and metastasis," *Nat. Cell Biol.*, vol. 10, no. 2, pp. 202–210, 2008.

[5] A. Esquela-Kerscher and F. J. Slack, "Oncomirs - MicroRNAs with a role in cancer," *Nat. Rev. Cancer*, vol. 6, no. 4, pp. 259–269, 2006.

[6] Y. Q. Liu, M. Zhang, B. C. Yin, and B. C. Ye, "Attomolar ultrasensitive microRNA detection by DNA-scaffolded silver-nanocluster probe based on isothermal amplification," *Anal. Chem.*, vol. 84, no. 12, pp. 5165–5169, 2012.

[7] Y. Long, L. F. Zhang, Y. Zhang, and C. Y. Zhang, "Single quantum dot based nanosensor for renin assay," *Anal. Chem.*, vol. 84, no. 20, pp. 8846–8852, 2012.

[8] C. M. Croce, "Causes and consequences of microRNA dysregulation in cancer," *Nat. Rev. Genet.*, vol. 10, no. 10, pp. 704–714, 2009.

[9] S. Catuogno, C. L. Esposito, C. Quintavalle, L. Cerchia, G. Condorelli, and V. de Franciscis, "Recent advance in biosensors for microRNAs detection in cancer," *Cancers (Basel).*, vol. 3, no. 2, pp. 1877–1898, 2011.

[10] C. Song, C. Zhang, and M. Zhao, "Rapid and sensitive detection of DNA polymerase fidelity by singly labeled smart fluorescent probes," *Biosens. Bioelectron.*, vol. 26, no. 5, pp. 2699–2702, 2011.

[11] K. A. Cissell and S. K. Deo, "Trends in microRNA detection," *Anal. Bioanal. Chem.*, vol. 394, no. 4, pp. 1109–1116, 2009.

[12] H.-L. Chen *et al.*, "Nucleic acid amplification-based methods for microRNA detection," *Anal. Methods*, vol. 7, no. 6, pp. 2258–2263, 2015.

[13] R. C. Lee, R. L. Feinbaum, and V. Ambros, "the C. elegans\rheterochronic gene lin-4 encodes small RNAs with antisense\rcomplementarity to lin-14.," *Cell* , vol. 75: 843–85, pp. 843–854, 1993.

[14] N. C. Lau, L. P. Lim, E. G. Weistein, and D. P. Bartel, "An abundant class of tiny RNA with probably regulatory roles in Caenorhabditis elegans," *Science (80-.).*, vol. 294, pp. 858–862, 2001.

[15] R. C. Lee and V. Ambros, "An extensive class of small RNA in Caenorhabditis elegans," *Science (80-.).*, vol. 294, pp. 862–864, 2001.

[16] Z. Mourelatos *et al.*, "miRNPs: A novel class of ribonucleoproteins containing numerous microRNAs," *Genes Dev.*, vol. 16, no. 6, pp. 720–728, 2002.

[17] B. Wightman, I. Ha, and G. Ruvkun, "Posttranscriptional regulation of the heterochronic gene lin-14 by lin-4 mediates temporal pattern formation in C. elegans," *Cell*, vol. 75, no. 5, pp. 855–862, 1993.

[18] A. E. Pasquinelli *et al.*, "Conservation of the sequence and temporal expression of let-7 heterochronic regulatory RNA," *Nature*, vol. 408, no. 6808, pp. 86–89, 2000.

[19] B. J. Reinhart *et al.*, "The 21-nucleotide let-7 RNA regulates developmental timing in Caenorhabditis elegans," *Nature*, vol. 403, no. 6772, pp. 901–906, 2000.

[20] S. Griffiths-Jones, "The microRNA Registry," *Nucleic Acids Res.*, vol. 32, no. 90001, p. 109D–111, 2004.

[21] S. Griffiths-Jones, "MiRBase: MicroRNA sequences and annotation," *Curr. Protoc. Bioinforma.*, vol. 34, no. SUPPL. 29, pp. 1291–12910, 2010.

[22] H. W. Hwang and J. T. Mendell, "MicroRNAs in cell proliferation, cell death, and tumorigenesis," *Br. J. Cancer*, vol. 94, no. 6, pp. 776–780, 2006.

[23] A. Grishok *et al.*, "Genes and mechanisms related to RNA interference regulate expression of the small temporal RNAs that control C. elegans developmental timing," *Cell*, vol. 106, no. 1, pp. 23–34, 2001.

[24] T. Kawamata, H. Seitz, and Y. Tomari, “Structural determinants of miRNAs for RISC loading and slicer-independent unwinding,” *Nat. Struct. Mol. Biol.*, vol. 16, no. 9, pp. 953–960, 2009.

[25] Y. Lee *et al.*, “The nuclear RNase III Drosha initiates microRNA processing,” *Nature*, vol. 425, no. 6956, pp. 415–419, 2003.

[26] A. C. E. Lung, S. Guttinger, “Science.pdf,” *Science (80-.).*, vol. 303, pp. 95–98, 2004.

[27] M. T. BOHNSACK, “Exportin 5 is a RanGTP-dependent dsRNA-binding protein that mediates nuclear export of pre-miRNAs,” *Rna*, vol. 10, no. 2, pp. 185–191, 2004.

[28] Y. Zeng and B. R. Cullen, “Structural requirements for pre-microRNA binding and nuclear export by Exportin 5,” *Nucleic Acids Res.*, vol. 32, no. 16, pp. 4776–4785, 2004.

[29] R. Yi, Y. Qin, I. G. Macara, and B. R. Cullen, “Exportin-5 mediates the nuclear export of pre-microRNAs and short hairpin RNAs,” *Genes Dev.*, vol. 17, no. 24, pp. 3011–3016, 2003.

[30] D. P. Bartel, “MicroRNAs: Genomics, Biogenesis, Mechanism, and Function,” *Cell*, vol. 116, no. 2, pp. 281–297, 2004.

[31] S. M. Hammond, “Dicing and slicing: The core machinery of the RNA interference pathway,” *FEBS Lett.*, vol. 579, no. 26, pp. 5822–5829, 2005.

[32] V. N. Kim, “Small RNAs just got bigger: Piwi-interacting RNAs (piRNAs) in mammalian testes,” *Genes Dev.*, vol. 20, no. 15, pp. 1993–1997, 2006.

[33] J. Halder *et al.*, “Focal adhesion kinasetargeting using in vivo short interfering RNA delivery in neutral liposomes for ovarian carcinoma therapy,” *Clin. Cancer Res.*, vol. 12, no. 16, pp. 4916–4924, 2006.

[34] J. G. Ruby *et al.*, “Large-Scale Sequencing Reveals 21U-RNAs and Additional MicroRNAs and Endogenous siRNAs in C. elegans,” *Cell*, vol. 127, no. 6, pp. 1193–1207, 2006.

[35] X. C. V. Ramachandran, “Degradation of microRNAs by a family of exoribonucleases in Arabidopsis.pdf,” *Science (80-.).*, vol. 321, pp. 1490–1492, 2008.

[36] S. Chatterjee and H. Großhans, “Active turnover modulates mature microRNA activity in Caenorhabditis elegans,” *Nature*, vol. 461, no. 7263, pp. 546–549, 2009.

[37] W. P. K. E. Wienholds, E. Miska, “MicroRNA expression development in zebrafish embyonic development,” *Science (80-.).*, vol. 309, pp. 310–311, 2005.

[38] M. N. Poy *et al.*, “pancreatic islet-speci c microRNA regulates insulin secretion,” *Nature*, vol. 432, no. November, pp. 226–230, 2004.

[39] R. M. O’Connell, D. S. Rao, A. A. Chaudhuri, and D. Baltimore, “Physiological and pathological roles for microRNAs in the immune system,” *Nat. Rev. Immunol.*, vol. 10, no. 2, pp. 111–122, 2010.

[40] H. F. Lodish, B. Zhou, G. Liu, and C. Z. Chen, “Micromanagement of the immune system by microRNAs,” *Nat. Rev. Immunol.*, vol. 8, no. 2, pp. 120–130, 2008.

[41] D. Baltimore, M. P. Boldin, R. M. O’Connell, D. S. Rao, and K. D. Taganov, “MicroRNAs: New regulators of immune cell development and function,” *Nat. Immunol.*, vol. 9, no. 8, pp. 839–845, 2008.

[42] S. J. Greco and P. Rameshwar, “MicroRNAs regulate synthesis of the neurotransmitter substance P in human mesenchymal stem cell-derived neuronal cells,” *Proc. Natl. Acad. Sci.*, vol. 104, no. 39, pp. 15484–15489, 2007.

[43] C. L. Jopling, M. Yi, A. M. Lancaster, S. M. Lemon, and P. Sarnow, “Modulation of Hepatitis C Virus RNA Abundance by a liver-specific MicroRNA,” vol. 309, no. September, pp. 1577–1581, 2005.

[44] S. Gilad *et al.*, “Serum microRNAs are promising novel biomarkers,” *PLoS One*, vol. 3, no. 9, pp. 1–7, 2008.

[45] M. Hanke *et al.*, “A robust methodology to study urine microRNA as tumor marker: MicroRNA-126 and microRNA-182 are related to urinary bladder cancer,” *Urol. Oncol. Semin. Orig. Investig.*, vol. 28, no. 6, pp. 655–661, 2010.

[46] N. J. Park *et al.*, “Salivary microRNA: Discovery, Characterization, and Clinical Utility for Oral Cancer Detection,” *Clin. Cancer Res.*, vol. 15, no. 17, p. 5473, 2009.

[47] S. Sassen, E. A. Miska, and C. Caldas, “MicroRNA - Implications for cancer,” *Virchows Arch.*, vol. 452, no. 1, pp. 1–10, 2008.

[48] G. A. Calin *et al.*, “Nonlinear partial differential equations and applications: Frequent deletions and down-regulation of micro- RNA genes miR15 and miR16 at 13q14 in chronic lymphocytic leukemia,” *Proc. Natl. Acad. Sci.*, vol. 99, no. 24, pp. 15524–15529, 2002.

[49] M. V. Iorio *et al.*, “MicroRNA gene expression deregulation in human breast cancer,” *Cancer Res.*, vol. 65, no. 16, pp. 7065–7070, 2005.

[50] J. A. Chan, A. M. Krichevsky, K. S. Kosik, J. A. Chan, A. M. Krichevsky, and K. S. Kosik, “MicroRNA-21 Is an Antiapoptotic Factor in Human Glioblastoma Cells MicroRNA-21 Is an Antiapoptotic Factor in Human,” no. 14, pp. 6029–6033, 2005.

[51] M. Jagla *et al.*, “A splicing variant of the androgen receptor detected in a metastatic prostate cancer exhibits exclusively cytoplasmic actions,” *Endocrinology*, vol. 148, no. 9, pp. 4334–4343, 2007.

[52] J.-F. Chen *et al.*, “Targeted deletion of Dicer in the heart leads to dilated cardiomyopathy and heart failure,” *Proc. Natl. Acad. Sci.*, vol. 105, no. 6, pp. 2111–2116, 2008.

[53] W. J. Lukiw, Y. Zhao, and G. C. Jian, “An NF-κB-sensitive micro RNA-146a-mediated inflammatory circuit in alzheimer disease and in stressed human brain cells,” *J. Biol. Chem.*, vol. 283, no. 46, pp. 31315–31322, 2008.

[54] T. Thum *et al.*, “MicroRNA-21 contributes to myocardial disease by stimulating MAP kinase signalling in fibroblasts,” *Nature*, vol. 456, no. 7224, pp. 980–984, 2008.

[55] C. Xiao and K. Rajewsky, “MicroRNA Control in the Immune System: Basic Principles,” *Cell*, vol. 136, no. 1, pp. 26–36, 2009.

[56] P. Varilly and D. Chandler, “NIH Public Access,” vol. v, no. 2, pp. 265–275, 2012.

[57] G. A. Calin *et al.*, “A MicroRNA signature associated with prognosis and progression in chronic lymphocytic leukemia.,” *N. Engl. J. Med.*, vol. 353, no. 17, pp. 1793–1801, 2005.

[58] A. Cimmino *et al.*, “miR-15 and miR-16 induce apoptosis by targeting BCL2,” *Proc. Natl. Acad. Sci.*, vol. 102, no. 39, pp. 13944–13949, 2005.

[59] F. Petrocca *et al.*, “E2F1-Regulated MicroRNAs Impair TGFβ-Dependent Cell-Cycle Arrest and Apoptosis in Gastric Cancer,” *Cancer Cell*, vol. 13, no. 3, pp. 272–286, 2008.

[60] F. Meng, R. Henson, H. Wehbe-Jane, K. Ghosal, S. T. Jacobs, and T. Patel, “MicroRNA-21 Regulates Expression of the PTEN Tumor Suppressor Gene in Human Hepatocellular Cancer,” *Gastroenterology*, vol. 133, no. 2, pp. 647–658, 2015.

[61] L. B. Frankel, N. R. Christoffersen, A. Jacobsen, M. Lindow, A. Krogh, and A. H. Lund, “Programmed cell death 4 (PDCD4) is an important functional target of the microRNA miR-21 in breast cancer cells,” *J. Biol. Chem.*, vol. 283, no. 2, pp. 1026–1033, 2008.

[62] C. Xiao *et al.*, “NIH Public Access,” *October*, vol. 9, no. 4, pp. 405–414, 2008.

[63] L. He, J. M. Thomson, M. T. Hemann, E. Hernando-monge, and D. Mu, “HHS Public Access,” vol. 435, no. 7043, pp. 828–833, 2015.

[64] B. P. Lewis, C. B. Burge, and D. P. Bartel, “Conserved seed pairing, often flanked by adenosines, indicates that thousands of human genes are microRNA targets,” *Cell*, vol. 120, no. 1, pp. 15–20, 2005.

[65] J. Krützfeldt *et al.*, “Silencing of microRNAs in vivo with ‘antagomirs,’” *Nature*, vol. 438, no. 7068, pp. 685–689, 2005.

[66] M. Scherr *et al.*, “Lentivirus-mediated antagomir expression for specific inhibition of miRNA function,” *Nucleic Acids Res.*, vol. 35, no. 22, 2007.

[67] D. Ovcharenko, K. Kelnar, C. Johnson, N. Leng, and D. Brown, "Genome-scale microRNA and small interfering RNA screens identify small RNA modulators of TRAIL-induced apoptosis pathway," *Cancer Res.*, vol. 67, no. 22, pp. 10782–10788, 2007.

[68] A. Esquela-Kerscher *et al.*, "The let-7 microRNA reduces tumor growth in mouse models of lung cancer," *Cell Cycle*, vol. 7, no. 6, pp. 759–764, 2008.

[69] J. Ji, J. Shi, and A. Budhu, "Regression of murine lung tumors by the let-7microRNA," vol. 29, no. 11, pp. 1580–1587, 2010.

[70] N. Kosaka, H. Iguchi, Y. Yoshioka, F. Takeshita, Y. Matsuki, and T. Ochiya, "Secretory mechanisms and intercellular transfer of microRNAs in living cells," *J. Biol. Chem.*, vol. 285, no. 23, pp. 17442–17452, 2010.

[71] Z. Liu, K. Chen, C. Davis, S. Sherlock, Q. Cao, and X. Chen, "NIH Public Access," vol. 68, no. 16, pp. 6652–6660, 2009.

[72] Q. X. Wang, J. Ren, X, "Nanoarchiteonic for smart Delivery and Drug Targeting Wang," *Science (80-.).*, vol. 3, pp. 940–945, 2008.

[73] N. W. S. Kam, Z. Liu, and H. Dai, "Functionalization of carbon nanotubes via cleavable disulfide bonds for efficient intracellular delivery of siRNA and potent gene silencing," *J. Am. Chem. Soc.*, vol. 127, no. 36, pp. 12492–12493, 2005.

[74] R. Singh *et al.*, "Tissue biodistribution and blood clearance rates of intravenously administered carbon nanotube radiotracers," *Proc. Natl. Acad. Sci.*, vol. 103, no. 9, pp. 3357–3362, 2006.

[75] A. Valoczi, "Sensitive and specific detection of microRNAs by northern blot analysis using LNA-modified oligonucleotide probes," *Nucleic Acids Res.*, vol. 32, no. 22, pp. e175–e175, 2004.

[76] C. Chen *et al.*, "Real-time quantification of microRNAs by stem-loop RT-PCR," *Nucleic Acids Res.*, vol. 33, no. 20, pp. 1–9, 2005.

[77] W. Li and K. Ruan, "MicroRNA detection by microarray," *Anal. Bioanal. Chem.*, vol. 394, no. 4, pp. 1117–1124, 2009.

[78] J. D. Driskell *et al.*, “Rapid microRNA (miRNA) detection and classification via surface-enhanced Raman spectroscopy (SERS),” *Biosens. Bioelectron.*, vol. 24, no. 4, pp. 917–922, 2008.

[79] D. Hanahan and R. A. Weinberg, “Hallmarks of cancer: The next generation,” *Cell*, vol. 144, no. 5, pp. 646–674, 2011.

[80] L. F. Sempere, S. Freemantle, I. Pitha-Rowe, E. Moss, E. Dmitrovsky, and V. Ambros, “Expression profiling of mammalian microRNAs uncovers a subset of brain-expressed microRNAs with possible roles in murine and human neuronal differentiation,” *Genome Biol.*, vol. 5, no. 3, p. R13, 2004.

[81] A. W. Wark, H. J. Lee, and R. M. Corn, “Multiplexed Detection Methods for Profiling microRNA Expression in Biological Samples,” *Angew Chem Int Ed.*, vol. 47, no. 4, pp. 644–652, 2008.

[82] D. A. Braasch and D. R. Corey, “Locked nucleic acid (LNA): fine-tuning the recognition of DNA and RNA.,” *Chem. Biol.*, vol. 8, no. 1, pp. 1–7, 2001.

[83] S. H. Ramkissoon, L. A. Mainwaring, E. M. Sloand, N. S. Young, and S. Kajigaya, “Nonisotopic detection of microRNA using digoxigenin labeled RNA probes,” *Mol. Cell. Probes*, vol. 20, no. 1, pp. 1–4, 2006.

[84] É. Várallyay, J. Burgyán, and Z. Havelda, “MicroRNA detection by northern blotting using locked nucleic acid probes,” *Nat. Protoc.*, vol. 3, no. 2, pp. 190–196, 2008.

[85] S. W. Kim *et al.*, “A sensitive non-radioactive northern blot method to detect small RNAs,” *Nucleic Acids Res.*, vol. 38, no. 7, pp. 1–7, 2010.

[86] J. S. H. Arlich, D. Gelfand, “sci.pdf,” *Science (80-.).*, vol. 252, pp. 1643–1651, 1991.

[87] P. M. Holland, R. D. Abramson, R. Watson, and D. H. Gelfand, “Detection of Specific Polymerase Chain-Reaction Product By Utilizing the 5’-]3’ Exonuclease Activity of Thermus-Aquaticus Dna-Polymerase,” *Proc. Natl. Acad. Sci. U. S. A.*, vol. 88, no. 16, pp. 7276–7280, 1991.

[88] J. Satsangi, D. P. Jewell, K. Welsh, M. Bunce, and J. I. Bell, “Effect of heparin on

polymerase chain reaction," *Lancet*, vol. 343, no. 8911, pp. 1509–1510, 1994.

[89] D. W. Hwang, I. C. Song, D. S. Lee, and S. Kim, "81-88 Smart magnetic fluorescent nanoparticle imaging probes to monitor MicroRNAs," *Small*, vol. 6, no. 1, pp. 81–88, 2010.

[90] R. Duan *et al.*, "Lab in a tube: Ultrasensitive detection of MicroRNAs at the single-cell level and in breast cancer patients using quadratic isothermal amplification," *J. Am. Chem. Soc.*, vol. 135, no. 12, pp. 4604–4607, 2013.

[91] G. L. Wang and C. Y. Zhang, "Sensitive detection of MicroRNAs with hairpin probe-based circular exponential amplification assay," *Anal. Chem.*, vol. 84, no. 16, pp. 7037–7042, 2012.

[92] T. Kilic *et al.*, "Electrochemical based detection of microRNA, mir21 in breast cancer cells," *Biosens. Bioelectron.*, vol. 38, no. 1, pp. 195–201, 2012.

[93] T. Tian, J. Wang, and X. Zhou, "A review: microRNA detection methods," *Org. Biomol. Chem.*, vol. 13, no. 8, pp. 2226–2238, 2015.

[94] J. Park and J.-S. Yeo, "Colorimetric detection of microRNA miR-21 based on nanoplasmonic core-satellite assembly.," *Chem. Commun. (Camb).*, vol. 50, no. 11, pp. 1366–8, 2014.

[95] B. C. Yin, Y. Q. Liu, and B. C. Ye, "One-step, multiplexed fluorescence detection of microRNAs based on duplex-specific nuclease signal amplification," *J. Am. Chem. Soc.*, vol. 134, no. 11, pp. 5064–5067, 2012.

[96] H. Lee, J. E. Park, and J. M. Nam, "Bio-barcode gel assay for microRNA," *Nat. Commun.*, vol. 5, p. 3367, 2014.

[97] M. Labib, N. Khan, S. M. Ghobadloo, J. Cheng, J. P. Pezacki, and M. V. Berezovski, "Three-mode electrochemical sensing of ultralow MicroRNA levels," *J. Am. Chem. Soc.*, vol. 135, no. 8, pp. 3027–3038, 2013.

[98] C. Li, Z. Li, H. Jia, and J. Yan, "One-step ultrasensitive detection of microRNAs with loop-mediated isothermal amplification (LAMP)," *Chem. Commun.*, vol. 47, no. 9, pp. 2595–2597, 2011.

[99] S. A. Oladepo and G. R. Loppnow, "Self-quenching smart probes as a platform for the detection of sequence-specific UV-induced DNA photodamage," *Anal.*

Bioanal. Chem., vol. 397, no. 7, pp. 2949–2957, 2010.

[100] O. Piestert *et al.*, "A single-molecule sensitive DNA hairpin system based on intramolecular electron transfer," *Nano Lett.*, vol. 3, no. 7, pp. 979–982, 2003.

[101] F. Li *et al.*, "Carbon nanotube-based label-free electrochemical biosensor for sensitive detection of miRNA-24," *Biosens. Bioelectron.*, vol. 54, pp. 158–164, 2014.

[102] Y. Zhou, Q. Huang, J. Gao, J. Lu, X. Shen, and C. Fan, "A dumbbell probe-mediated rolling circle amplification strategy for highly sensitive microRNA detection," *Nucleic Acids Res.*, vol. 38, no. 15, p. e156, 2010.

[103] Y. Zhao, L. Zhou, and Z. Tang, "Cleavage-based signal amplification of RNA," *Nat. Commun.*, vol. 4, pp. 1493–1498, 2013.

[104] H. Jia, Z. Li, C. Liu, and Y. Cheng, "Ultrasensitive detection of microRNAs by exponential isothermal amplification," *Angew. Chemie - Int. Ed.*, vol. 49, no. 32, pp. 5498–5501, 2010.

[105] T. Heinlein, J.-P. Knemeyer, O. Piestert, and M. Sauer, "Photoinduced Electron Transfer between Fluorescent Dyes and Guanosine Residues in DNA-Hairpins," *J. Phys. Chem. B*, vol. 107, no. 31, pp. 7957–7964, 2003.

[106] N. Marmé and J. P. Knemeyer, "Sensitive bioanalysis-combining single-molecule spectroscopy with mono-labeled self-quenching probes," *Anal. Bioanal. Chem.*, vol. 388, no. 5–6, pp. 1075–1085, 2007.

[107] D. D. Taylor and C. Gercel-Taylor, "MicroRNA signatures of tumor-derived exosomes as diagnostic biomarkers of ovarian cancer," *Gynecol. Oncol.*, vol. 110, no. 1, pp. 13–21, 2008.

[108] S. Tyagi and F. R. Kramer, "Molecular Beacons: Probes that Fluoresce Upon Hybridization," *Nat. Biotechnol.*, vol. 14, no. 3, pp. 303–308, 1996.

[109] G. Bonnet, S. Tyagi, A. Libchaber, and F. R. Kramer, "Thermodynamic basis of the enhanced specificity of structured DNA probes.," *Proc. Natl. Acad. Sci. U. S. A.*, vol. 96, no. 11, pp. 6171–6, 1999.

[110] K. Stöhr, B. Häfner, O. Nolte, J. Wolfrum, M. Sauer, and D. P. Herten, "Species-specific identification of mycobacterial 16S rRNA PCR amplicons using smart

probes," *Anal. Chem.*, vol. 77, no. 22, pp. 7195–7203, 2005.

[111] A. Misra, P. Dwivedi, and M. Shahid, "A probe for detection of G-rich target strands through fluorescence quenching," *Russ. J. Bioorganic Chem.*, vol. 35, no. 1, pp. 62–67, 2009.

[112] J. P. Knemeyer, N. Marmé, and M. Sauer, "Probes for detection of specific DNA sequences at the single-molecule level.," *Anal. Chem.*, vol. 72, no. 16, pp. 3717–3724, 2000.

[113] S. Steenken and S. V. Jovanovic, "How easily oxidizable is DNA? One-electron reduction potentials of adenosine and guanosine radicals in aqueous solution," *J. Am. Chem. Soc.*, vol. 119, no. 3, pp. 617–618, 1997.

[114] J. Pan, Y. Zhang, J. Xu, J. Liu, L. Zeng, and G.-M. Bao, "A smart fluorescent probe for simultaneous detection of GSH and Cys in human plasma and cells," *RSC Adv.*, vol. 5, no. 118, pp. 97781–97787, 2015.

[115] G. Zhu, L. Liang, and C. Y. Zhang, "Quencher-free fluorescent method for homogeneously sensitive detection of micrornas in human lung tissues," *Anal. Chem.*, vol. 86, no. 22, pp. 11410–11416, 2014.

[116] Q. Xi *et al.*, "Highly sensitive and selective strategy for microRNA detection based on WS2nanosheet mediated fluorescence quenching and duplex-specific nuclease signal amplification," *Anal. Chem.*, vol. 86, no. 3, pp. 1361–1365, 2014.

[117] P. P. Sengupta, "A Platform for Fast Detection of Let-7 Micro RNA Using Polyaniline Fluorescence and Image Analysis Techniques," 2015.

[118] H. H. Zhang, X. J. Wang, G. X. Li, E. Yang, and N. M. Yang, "Detection of let-7a microRNA by real-time PCR in gastric carcinoma," *World J. Gastroenterol.*, vol. 13, no. 20, pp. 2883–2888, 2007.

[119] G. Leone, H. Van Schijndel, B. Van Gemen, F. R. Kramer, and C. D. Schoen, "Molecular beacon probes combined with amplification by NASBA enable homogeneous, real-time detection of RNA," *Nucleic Acids Res.*, vol. 26, no. 9, pp. 2150–2155, 1998.

[120] A. F. El-Yazbi and G. R. Loppnow, "Chimeric RNA-DNA molecular beacons for quantification of nucleic acids, single nucleotide polymophisms, and nucleic acid damage," *Anal. Chem.*, vol. 85, no. 9, pp. 4321–4327, 2013.

Vitae

Name	:Yusuf Basiru Olayinka
Nationality	:Nigeria
Date of Birth	:10/22/1986
Email	:yusufbashir2@yahoo.com
Address	:No 2 Fadare Close Iwo Road, Ibadan, Oyo State, Nigeria.
Postal Address	P.O Box 11194 Dugbe Ibadan, Oyo State, Nigeria.
Academic Background	: Bachelor of Science in Industrial Chemistry
List of Pubications:	Basiru O. Yusuf and Sulayman A. Oladepo. Development of smart probe detection platform for cancer diagnosis.To be Submitted in Journal Applied Spectroscopy.